DESIGN OF MEMS BASED MICROHEATER FOR EFFICIENT GAS SENSOR

Thesis report submission in the partial fulfillment of the

Requirement for the award of the degree of

MASTERS OF TECHNOLOGY

IN

VLSI DESIGN

Submitted by

Mayank Dhull

Roll No: 601361012

Under the Guidance of

Dr. Anil Arora

Assistant Professor, ECED

DEPARTMENT OF ELECTRONICS AND COMMUNICATION

ENGINEERING

THAPAR UNIVERSITY, PATIALA (PUNJAB) – 147004

JULY-2015

CERTIFICATE

I hereby declare that the work which is being presented in the thesis entitled "**Design of MEMS based microheater for efficient gas sensor**" in partial fulfillment of the requirement for the award of degree of M.Tech. (VLSI Design) at Electronics and Communication Engineering Department of Thapar University, Patiala, is an authentic record of my own work carried out under the supervision of Dr. Anil Arora, Assistant Professor, ECED.

The matter presented in this thesis has not been submitted in any other University/Institute for the award of my degree.

Date: 10/7/2015

Mayank Dhull

Roll No: 601361012

It is certified that the above statement made by the student is correct to the best of my knowledge and belief.

10/7/15

Dr. Anil Arora

Assistant Professor

ECED, Thapar University

Counter signed by:

Dr. Sanjay Sharma

Professor & Head

ECED, Thapar University

Patiala-147004

Dr. S. S. Bhatia

Dean of Academic Affairs

Thapar University

Patiala-147004

ACKNOWLEDGEMENT

I take this opportunity to express my profound sense of gratitude and respect to all those who helped me through the duration of this thesis. I would have never succeeded in completing my task without the cooperation, encouragement and help provided to me by various people. Words are often too less to reveal one's deep regards. I acknowledge with gratitude and humility my indebtedness to **Dr. Anil Arora, Assistant Professor**, Electronics and Communication Engineering Department, Thapar University, Patiala, under whose guidance I had the privilege to complete this thesis. I wish to express my deep gratitude towards him for providing individual guidance and support throughout the thesis work.

I convey my sincere thanks to **HEAD OF THE DEPARTMENT, Dr. Sanjay Sharma,** Electronics and Communication Engineering Department, entire faculty and staff of Electronics and Communication Engineering Department for their encouragement and cooperation. I am also thankful to **PG Coordinator, Dr. Amit Kumar Kohli** for his support and wishes.

My greatest thanks to all who wished me success especially my parents and other family members and friends without whom I would not have been able to complete my thesis work.

I thank and own my deepest regards to all of them and all others who have helped me directly or indirectly.

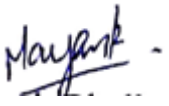

Mayank Dhull

ABSTRACT

A sensor, originates from the Latin word “SENTIRE”, is a device, which perceives and responds to a physical and chemical stimulus. Semiconductor sensors are such type of electronic devices in which the semiconducting material is responsible for sensing function. Micro-Electromechanical Systems (MEMS) based integrated gas sensors present several advantages for these applications such as array fabrication, small size, and unique thermal manipulation capabilities. MEMS based gas sensors, which are usually produced using a standard CMOS (Complementary Metal Oxide Semiconductor) process, have the additional advantages of being readily realized by commercial foundries and amenable to the inclusion of on-chip electronics.

Gases are linked to life and their odors tremendously influence the image of our environment. The human nose serves as a highly advanced sensing instrument which is able to differentiate between hundreds of smells but fails if absolute gas concentrations or odorless gases need to be detected. The demand for gas sensing devices which support the human nose is accordingly large. Support is desired in safety applications where combustible or toxic gases are present and in comfort applications, such as climate controls of buildings and vehicles where good air quality is required. Additionally, gas monitoring is needed in process control and laboratory analytics.

Most of the microheaters which are used to elevate the temperature of gas sensor, integrated with the design of either platinum, nichrome or poly-silicon etc. as heater element are suitable for high temperatures and were fabricated with poly-silicon as heater material as well as electrode to observe the particular ambient temperature. In the present work, a platinum based coplanar microheater is designed and studied for gas sensing applications. Microheaters with different structures are designed to obtain better temperature uniformity. Interdigitated electrodes can be placed on the same layer as of microheater to obtain a coplanar design. The design has been accomplished using finite element method (FEM) through COMSOL Multiphysics.

CONTENTS

LIST OF FIGURES PAGE NO.

LIST OF TABLES PAGE NO.

ABBREVIATIONS

MEMS	Micro Electro Mechanical System
IDT	Interdigitated Transducer
IDE	Interdigitated Electrodes
CVD	Chemical Vapor Deposition
PVD	Physical Vapor Deposition
ICs	Integrated Circuits
Poly-Si	Poly silicon
Pt	Platinum

CHAPTER-1

INTRODUCTION

Gas sensors are used to determine the information about gases present in the atmosphere. MEMS based gas sensors have the advantage of small size and low power consumption. A gas sensor consists of a sensing layer/film which is sensitive to the presence of gas. Sensing layer used is generally oxides or metal oxides. Gas sensor operates generally in the temperature range of ~150℃ to 300 ℃. Microheater is used to heat the sensing layer so that the gas present in the environment can react with the sensing layer. Interdigitated Transducer (IDT) is used to measure the change in resistivity of the sensing layer in the form of resistance change across the IDT terminals.

1.1 MEMS: An Introduction

MEMS stands for Micro Electro Mechanical System. MEMS devices are micro level devices having both electrical and mechanical components. Generalized definition of MEMS is "It is a device where micro sensor and mechanical parts (Actuators) along with signal processing circuitry are combined on very tiny slice of silicon". MEMS devices are fabricated using IC compatible batch process techniques. Materials like silicon, quartz, glass and polymer can be used as substrate in these devices [1].

MEMS is based on three basic blocks- sensor, processor and actuator as shown in Fig. 1.1. Sensor or micro-sensor senses the measurand or input signal. Most of time input is probably non - electrical signal which is converted into electrical signal by a transducer. Vectorial representation of a sensor is shown in Fig. 1.2(a). Processor is next to sensor block which gets electrical signal from sensor. Processor is used to perform mathematical or logical operations on the signal. Processor has electrical signal as input and output. The final building block is the actuator which gets electrical signal from the processor as input and generally gives a non-electrical signal as output.

Vectorial representation of an actuator is shown in Fig.1.2(b). Actuator actually responds to environment (e.g. pumping, filtering, positioning, regulating and moving) based on intended designed instruction [2].

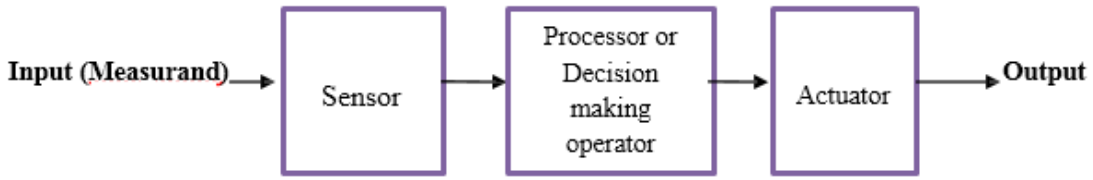

Fig. 1.1 Basic block diagram of MEMS.

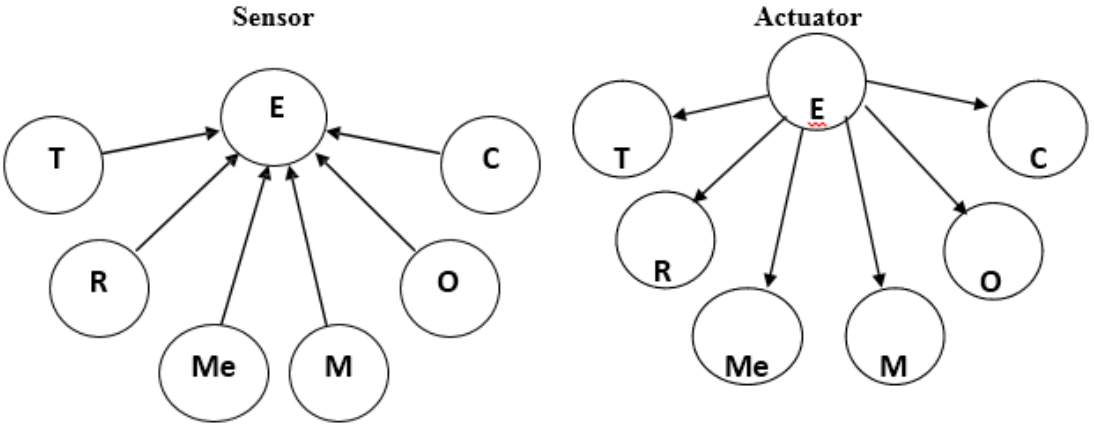

(a) (b)

Fig. 1.2 Vectorial representation of (a) sensor (b) actuator in energy domain space.

Where, E-Electrical, T-Thermal, R-Radiation, Me-Mechanical, M-Magnetic, O-Optical, C – Chemical.

The real power of this technology is that many devices can be built at the same time across the surface of the wafer, with no assembly required. Since it is a photographic-like process, its just as easy to build a million devices on the wafer as it would be to build just one. MEMS promises to revolutionize nearly every product category by bringing together silicon-based microelectronics with micromachining technology, making possible the realization of complete systems-on-a-chip. MEMS is an enabling technology allowing the development of smart products, augmenting the

computational ability of microelectronics with the perception and control capabilities of microsensors and microactuators and expanding the space of possible designs and applications.

For fabrication of MEMS, three processing steps are used: (1) Deposition (2) Lithography and (3) Etching. In deposition, thin films of material are deposited on substrate. Chemical reaction method and physical reaction method are used for deposition. Chemical reaction methods which are like, chemical vapor deposition (CVD), Electro deposition, epitaxy and thermal oxidation. The physical reaction methods which are like, physical vapor deposition (PVD) and casting. In lithography, a patterned mask is applied on top of the film by photolithographic imaging. It can be classified in two groups: (1) Pattern transfer and (2) Lithographic module. In etching process, it is necessarily requirement to etch the films selectively to the mask. Basically, it is subdivided in two methods: dry etching and wet etching.

One common MEMS (Micro-Electro Mechanical Systems) fabrication technique is the anisotropic etching of crystalline silicon, where etch rate is a function of orientation. The anisotropic etching of silicon is ubiquitous process in micromachining. Complex microsystems can be generated using the anisotropic properties of single crystal silicon in an orientation dependent dissolution reaction. Modern exacting demands in this rapidly growing industry require fundamental understanding of these processes in order to achieve a well-defined anisotropic ratio and a good surface finish. Mostly used technology for bulk structuring for micro sensors and actuators is the anisotropic etching with KOH. Specifications for the etched structures (such as high etch rate ratios of <110> and <100> to <111> planes, short etch times and minimum roughness) can be obtained by optimization of the etch parameters. For sensor applications <100> oriented silicon is mostly used. Advantages and disadvantages of the different etching conditions are anisotropic direction selectivity, speed and surface roughness of the pattern. In isotropic etching, all orientations or planes etch at the same rate, hence a square hole would get rounded corners. In anisotropic etching, because of the differences in rates some planes grow while others disappear. There are two main classifications that describe how the initial mask shape will evolve into the final etched shape.

Firstly, etched shapes may be classified as either pegs or holes. Holes are lower than the surface of the wafer and pegs are higher than the wafer, Holes enlarge with time while pegs shrink.

1.2 History of MEMS

MEMS was first developed in the 1970s and then it was commercialized in 1990s. Using MEMS, it becomes possible to make any system to be smaller, more efficient, less expensive and faster. In an ideal MEMS configuration, ICs (Integrated Circuits) provide the "thinking" part of that system, while MEMS supplement this intelligence with control functions and perception [3]. Pressure sensors having bulk etched silicon structure were the first wave of MEMS commercialization started in the late 1970s and early 1980s. In that first pressure sensor silicon membrane deformed under pressure and piezoresistive track laid on its surface, was affected and the change is used to transform the pressure into an electronic signal [4].

A second wave of commercialization arrived in the 1990s, which was mainly focused on information technology and personal computers (PCs). In this era, video projection is one of the products that was introduced by Texas Instrument which is depended on electrostatic actuated tilting micro mirror arrays. There is another product named thermally operated inkjet print head that remain a high demand application till date.

A micro-optics as an accompaniment to optical fiber communication - by way of all optical related devices and optical switches is the third generation of MEMS commercialization [5]. And the fourth wave of the commercialization could be other applications that may include biological and neural probes, also called lab-on-chip drug development and biochemical system and macro scale drug delivery system. E-nose is also the latest application that comes under fourth generation of MEMS commercialization.

1.3 MEMS Material

MEMS technology may be implemented using different manufacturing techniques and different materials that totally depends on the device which is being created and the market in which it has to operate [6]. Different types of materials are:

Silicon

It is the material which is widely used in consumer electronics. It has very suitable material properties among other choices like; it can survive in harsh conditions, has uniform mechanical properties throughout the wafer lots, and also has suitable mechanical, thermal, electrical and optical integration. In a form of single crystal, silicon is considered as almost perfect example of Hookean material, that when it is flexed, there is almost no energy dissipation because it has virtually no hysteresis. Also silicon has very high reliability as this material suffers very little fatigue and also has service lifetime in the range of billions to trillions. And the biggest advantage is fabrication and treatment processes for silicon substrate are documented and well established. Also silicon compounds are also used in MEMS. Some of the examples are Silicon dioxide (SiO_2), Poly-Silicon (Poly-Si), Silicon Carbide (SiC) and Silicon Nitride (Si_3N_4).

Quartz

It is basically a compound of Silicon dioxide (SiO_2) and its orientation is not based on Miller indices. It is also counted as an ideal choice of material for MEMS sensor as it has near absolute thermal dimensional stability. It is advisable material in case of micro fluidics applications in biomedical analysis. It has certain advantages over silicon that it is more dimensionally stable, more flexible in geometry and transparent to ultraviolet light which is better for motive of species detection.

Gallium Arsenide

It is compound semiconductor and is a major candidate for photonics devices as it has high mobility of electrons. It is higher level thermal insulator having outstanding dimensional stability at high temperature. In comparison to silicon it is more difficult to process and more expensive.

Polymers

They are nowadays become popular choice for MEMS and micro system

though having biggest drawback of poor conductivity. They have certain proficient advantages like, low cost of raw material, light weight, high electrical resistance.

Metals

Metals are used to make MEMS elements. Although metals do not have the advantages that are displayed by silicon but in terms of mechanical properties, it shows high reliability. Widely used metals are platinum, gold, aluminum, silver, copper.

1.4 Advantages of MEMS

- Miniaturization: Smaller size, low power consumption, ruggedness.
- IC Compatible: Higher performance.
- Batch Fabrication: Low cost.
- Low power consumption.

1.5 Application of MEMS

MEMS devices are often found as sensors like gas sensors, pressure sensors, optical sensors, position and speed micro sensors and is also making large inroads into defense, medical, aviation, optical communication [2,3] and many more.

a) Communication

It is more benefiting to make high frequency circuits with the help of RF-MEMS technology. Electrical components like, tunable capacitors and inductors can be enhanced remarkably using MEMS technology. The total circuit area, cost and power consumption can be decreased and the performance of communication circuits can be enhanced if the proper integration of such components are made perfectly. RF-MEMS is widely used in antennas, oscillators, phase shifter circuits and filters.

b) Biotechnology

For DNA identification and amplification, MEMS is providing new discoveries in engineering and science like the Polymerase Chain Reaction (PCR)

system. Also there are micro-systems for throughput drug selection and drug screening, micro- machined Scanning Tunneling Microscopes (STMs). For detection of hazardous biological agents and chemical agents, biochips are developed. Bio-MEMS in health and medical related technologies, one important development of Lab-On-Chip for chemo sensor and biosensor is made.

c) Integrated Circuits

Micro technology generally has been developed for producing silicon semiconductor. The revolution in silicon has allowed to create reliable, small processor in form of IC (Integrated Circuits). Micro-machined substrates are having significant importance for low power pressure sensors, temperature sensor, gas sensors etc.

d) Automotive Domain

MEMS devices are widely used in airbag system, active suspension and automatic door lock system. They have large applications in vehicle security systems, headlight leveling systems and inertial brake lights. MEMS sensors are having application in air temperature control in cars.

1.6 Concept of Electronic-Nose (E-nose)

In many industries, for measurement of quality of perfumes, drinks, foods and sometimes chemical and cosmetic products, the human nose is used as diagnostic tool [7]. Human sensory panels are highly subjective as human smell estimation is affected by many factors. These individual variations may occur and also be affected by mental health and physical health [8]. One of the great achievement and application of MEMS is E-nose. E-nose is a device which imitates the discrimination of the mammalian olfactory system which is sensory system for smell [9].

The E-nose has sensor arrays which act as olfactory system of human nose that have number of sensing sense [10]. The odor samples sense on the array sensing surface causes a chemical and/or physical change on that surface which changes associated electrical properties of sensing surface like, conductivity or current.

1.6.1 E-nose sensor response to odorants

E-nose sensor's response to odorants is normally observed as a 1st order time response. In the very first stage of odor testing, it is necessary to acquire a baseline by flushing a reference gas by sensor. When it is exposed to that odorant, it causes variations in output signal till the sensor attains to steady-state value. Finally the odorant is removed from the sensor by using the help of reference gas and it comes back to its original baseline value. Here this process gives two important definitions.

Response time: It is the time taken by for the sensor to sense (expose) the odorant.

Recovery time: It is the time taken by sensor to come back to its baseline resistance value. The succeeding stage in this odor analysis is sensor response manipulation that is obviously with respect to baseline value and this process reduces drift, noise and also naturally generated large or small signals [8].

Some common sensors used for E-nose are:

- **Intrinsically conducting sensor:** When vapor / gas is flushed on surface of conducting polymers, conducting polymers expand and its resistance will be changed that cause change in conductivity.
- **Composite Conducting polymers sensor:** They have combinations of conducting polymer and non-conducting particles. Typically conducting polymers like, carbon black and polypyrrole (PPy) scattered in an insulating polymer matrix.
- **Surface acoustic wave (SAW) sensor:** In surface acoustic wave sensor, input transducer, gas sensitive coating and output transducer is deposited on piezoelectric substrate. As input transducer gets ac input, it generate acoustic wave. There is change in mass of gas sensing membrane that causes alteration of acoustic frequency produced by input transducer. This change is observed by output transducer.
- **Quartz crystal microbalance sensor:** It works on same principle as SAW sensor. Normally, piezoelectric material oscillates while ac supply voltage is applied and it produces resonance frequency. But gas is absorbed by this material and it changes its mass and that makes change in resonance

frequency.

- **Optical sensors:** Glass fiber coated with dye saturated polymer is used for sensing purpose. At one end of fiber, light is entered with original wavelength and due to gas interaction of fiber at the other end, the shift in wavelength is observed.
- **Metal oxide field effect transistor (MOSFET) sensors:** The basic concept of metal oxide field effect transistor (MOSFET) sensor is that there is variation in oxide conduction while it interacts with a gas. Also this variation normally proportional to the amount of gas concentration.

1.6.2 Applications of E-nose sensor

E-nose has countless applications in many areas such as food products, agriculture field, medical field, military etc. All these applications are explained as below.

1. **Agriculture Field:** E-nose is used in crop protection, plant production, to find plant harvest timing, to find crop (fruit) ripeness, to find pre & post-harvest diseases, pest identification [11].

2. **Pharmaceutical and Medical:** Its applications are in product purity checking, quality control of drugs, consistency and uniformity of drug formulation, cancer detection, Urinary Tract Infections (UTI) detection, respiratory diseases recognition and other clinical discovery [12,13].

3. **Manufacturing:** E-nose is widely applicable in hazardous gas leak detection, to inspect flavor and aroma, safety & security, examine manufacturing process [11].

4. **Food & Beverage:** It is utilized in product variety analysis, product evenness checking, smell reorganization, quality assessment, smell characteristics checking, milk (dairy) product checking, meat and sea food quality checking etc [11,14].

5. **Military:** Explosive substance detection, military and civilian safety and

security, also chemical and biological weapons detection etc. are applications of E-nose in military [15].

6. **Environment:** It is used in hazardous gas identification, pollution detection, water & air quality checking etc. [16,17]

7. **Aroma and Cosmetics:** Its application may be in **c**omparing natural and artificial cosmetic products, to measure efficiency of deodorants, to find life time of perfume etc. [15].

1.7 Metal Oxide Gas Sensor

Although we have already discussed all options for gas sensor used in E-nose in topic 1.2.1, metal oxide sensor is the best option as it has certain advantages as mentioned below [16].

- Easy electronic interface
- Capability to detect no. of gases
- Ease of use
- Very low maintenance
- Good sensitivity
- Low cost
- Fast response time

There are two available options of MOSFET sensors. One is n-type sensors (sensing surface) which have majority charge carriers as electrons such as ZnO (Zinc Oxide), TiO_2 (Titanium dioxide), WO_3 (Tungsten trioxide), Fe_2O_3 (Iron (III) oxide) etc. While another is p-type sensors (sensing surface) having holes as majority charge carriers such as NiO_2 (nickel oxide), CoO (cobalt oxide) and others. MOSFET sensors surface is highly sensitive with oxidizing gases (such as N_2O, CO_2, NO_2, and NO etc.) which cause increase in depletion region of sensing surface and reducing gases (such as NH_3, CH_4, SO_2, H_2S and CO etc.) which cause decrease in depletion region of sensing surface [16]. This slight change of depletion region causes electrical properties of material from that amount (concentration) of certain gas can be measured.

1.8 Need of Micro-Heater

In metal oxide sensor, which uses electron depleted surface, either oxidation or reduction process occur on depleted sensing surface or oxide surface. In these process electrons are added or extracted depending on metal oxide sensor whether is n-type or p-type. But all these process generates oxygen. It needs very high temperature (around 100^{o} C to 600^{o} C) to occur this phenomena depending upon the gases and used sensing surfaces.

To achieve this high temperature in metal oxide sensor, there is a need of micro- heater (sometimes it called as heating element or heater). The main task of micro-heater is to provide temperature uniformity (with attaining constant high temperature) for sensing layer. Also micro-heater must operate at less applied voltage so power consumption can be reduced. If micro-heater is in direct contact with substrate, it may damage substrate. So generally, micro-heater is placed on platform of SiO_2 (Silicon dioxide).

1.9 Structure of metal oxide based gas sensor

In any metal oxide based gas sensor structure has basically five layers (as shown in Fig. 1.3):

- Substrate
- Insulating platform
- Micro-heater
- Interdigitated electrodes
- Sensing Film

Substrate:

Silicon is considered as the best choice as substrate in all the integrated circuits, all the electronic consumer products and MEMS as well due to its various advantages as already discussed in previous section.

Insulating platform:

To give electrical insulation, a thin layer of SiO_2 (Silicon dioxide) or sometime Si_3N_4 (Silicon Nitride) is used. This is helpful to avoid direct damage on substrate due temperature from 100^{o} C to 600^{o} C, generated because of heating of

microheater.

Micro-heater:

MEMS based metal oxide structure is very small in terms of surface (around some hundreds of μm^2 surface area). Microheater is critical component of metal oxide gas sensor to detect the desired gas properly. As micro-heater geometry in the range of micron dimension, it requires very low applied voltage to achieve very high temperature. The heating of micro-heater is based on joule heating concept. Micro-heaters are extensively used in humidity sensors, microfluidics, gas sensors and many other micro systems.

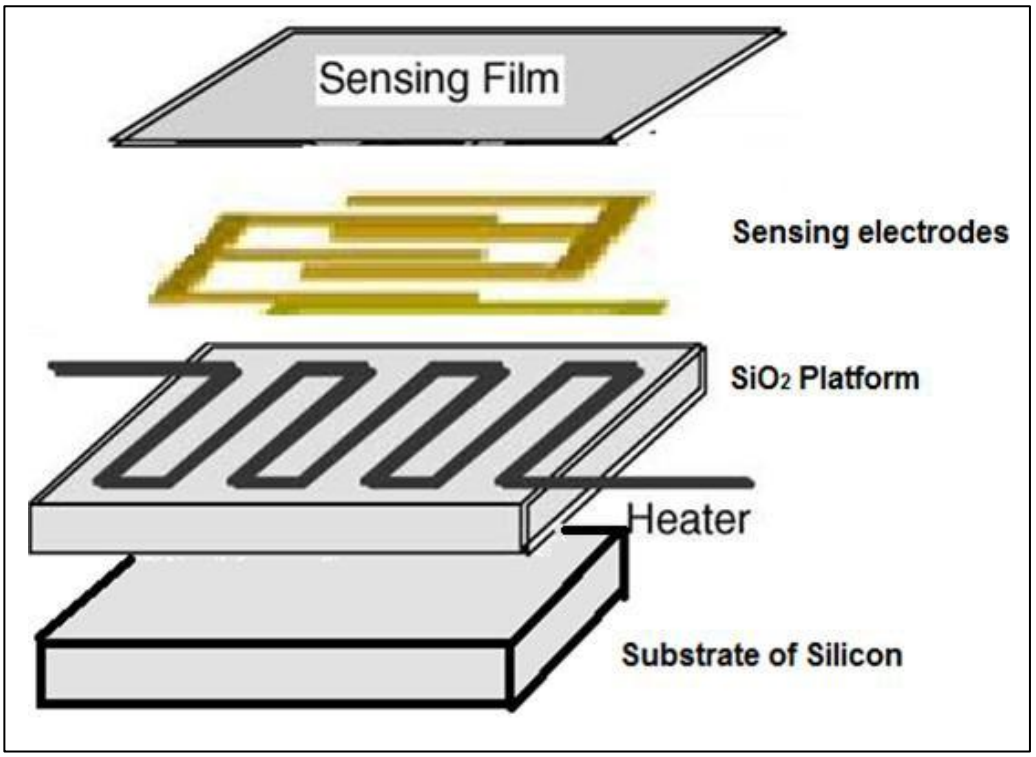

Fig. 1.3 Basic structure of metal oxide based gas sensor.

Interdigitated electrodes:

On the SiO_2 platform, micro-heater is placed and interdigitated electrodes made of aluminum, gold or platinum is placed coplanar to the heater, which detect variations in resistance of metal oxide sensing surface while it responds to gases. The term *interdigitated,* selected for use throughout this,

refers to a digitlike or fingerlike periodic pattern of parallel in-plane electrodes used to measure the resistance when a gas is present on the material sample or sensitive coating. A typical chemical interdigitated sensor design is to deposit interdigitated electrodes on an insulating substrate. The electrodes are coated with a thin layer of material that is sensitive to the concentration of chemicals present in the ambient atmosphere. The most common outputs of measurement are changes in resistance and capacitance between electrodes. The sensing mechanism is that when the sensor is exposed to ambient chemicals, the interaction of the chemicals with the sensitive material coating changes the material's conductivity, dielectric constant, and/or the effective thickness of the sensitive layer. The change in conductivity and effective thickness result in a resistance change, and the change of dielectric constant and effective thickness of the sensitive layer changes the capacitance. Interdigitated chemical sensors are inexpensive to manufacture and can be integrated on a chip consisting of the sensor element and signal processing electronics. Fig. 1.4 shows a microheater design with coplanar IDT [49].

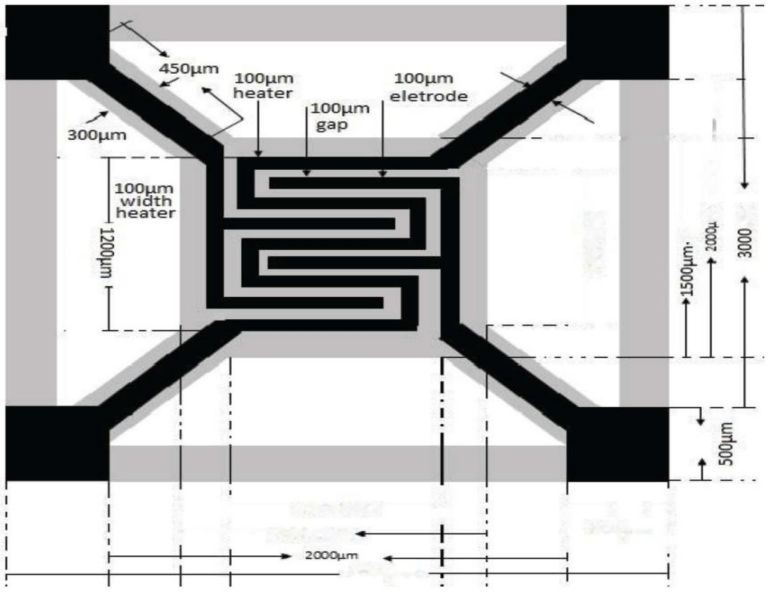

Fig.1.4 Microheater integrated with IDT [49]

Metal oxide sensing layer:

There are several options available for metal oxide sensing layer. The concentration of any gases on the sensing surface is measured in terms of ppm (part per million) or ppb (part per billion). The resistivity / conductivity of sensing surface changes with amount of gas concentration. The temperature limit of some selected metal oxide sensing surface are shown in Table 1.1 [19].

Table 1.1 Temperature limit of some selected metal oxide sensing surfaces used in gas sensors.

Sr. No.	Metal Oxides sensing surface	Temperature limit/ range
1	Tin oxide (SnO_2)	300° C or above
2	Zinc oxide (ZnO)	300° C
3	Tungsten trioxide (WO_3)	Up to 500° C
4	Indium tin oxide (ITO)	300° C
5	Titanium oxide (TiO_2)	250° C
6	Cerium oxide (CeO_2)	400° C

As metal oxides have very good sensitivity to some hazardous gases, used for sensing purpose. Some typical metal oxide sensing surface and aimed gases are shown in Table 1.2 [16,20].

Table 1.2 Typically used metal oxide sensing surface and their aimed gases.

Sr. No.	Metal Oxides sensing surfaces	Aimed gas
1	Tungsten trioxide (WO_3), Zinc oxide (ZnO)	Nitrogen dioxide (NO_2)
2	Tungsten trioxide (WO_3)	Nitric oxide (NO)
3	Tin oxide (SnO_2), Zinc oxide (ZnO)	Nitrous oxide (N_2O)
4	Tungsten trioxide (WO_3), Zinc oxide (ZnO)	Hydrogen sulfide (H_2S)
5	Zinc oxide (ZnO), Titanium oxide (TiO_2)	Carbon monoxide (CO)
6	Titanium oxide (TiO_2), Tin oxide (SnO_2)	Ammonia (NH_3)
7	Tungsten trioxide (WO_3), Tin oxide (SnO_2), Zinc oxide (ZnO)	Methane (CH_4)
8	Tungsten trioxide (WO_3), Zinc oxide (ZnO), Tin oxide (SnO_2)	Sulfur dioxide (SO_2)
9	Zinc oxide (ZnO), Tin oxide (SnO_2)	Carbon dioxide (CO_2)

CHAPTER-2

LITERATURE REVIEW

2.1 Literature Review

The focus of this work is to design a microheater for gas sensing application. They have good sensitivity to some relevant gases like CO, H2, NOx and hydrocarbons. Metal oxide gas sensors are frequently used in gas leakage detection (propane, butane) and ambient air quality monitoring (CO, NOx). New application fields are toxic gas detection like CO and smoke gas monitoring in houses and buildings. In a semiconductor gas sensor, a micro-heater is used as a hot plate which controls the temperature of the sensing layer. The semiconductor gas sensor utilizes semiconductor properties of surface adsorption which is used to detect changes in resistance as a function of varying concentrations of different gases. In order to detect these resistive changes, the heater temperature must be held constant and uniform over the heater area. Therefore, sensitivity, selectivity and response time of the semiconductor gas sensor are dependent on the sensing layer material and operating temperature of the micro-heater [21]. Use of a micro-heater is important in gas sensors because the gas reaction in the sensing layer occurs at high temperatures. Materials used in metal oxide gas sensors are SnO2, ZnO, TiO2, and WO3. All those materials are n-type semiconductors, which have, typical working temperature in the range 200-600 K [22-23]. In a gas sensor, microheater is used to control the temperature of the sensing layer. The idea of using semiconductors as gas sensitive devices leads back to1952 when Brattain and Bardeen first reported gas sensitive effect on germanium [23]. Later Siyanda, found gas sensing effect on metal oxides [24]. Taguchi finally brought semiconductor sensors based on metal oxides to an industrial product [23]. Taguchi type sensors are still in the market, but most of the commercially available sensors are manufactured in screen printing technique on small and thin ceramic substrates [23, 25, 26]. Screen printing technique has the advantage that thick film of metal oxide semiconductor sensor are deposited in batch processing thus leading to a small sensor to sensor distribution within production lots. However, screen-printed ceramic gas sensors are, with respect to power consumption, mounting technology and selectivity still in need of improvement. The power consumption of screen printed devices is typically in the range of 1-5 Watt

[25] that is too much for application which allow just the use of battery driven elements. The mounting of the overall hot ceramic element is difficult. One has to find such designs that ensure good thermal insulation between sensor element and housing as well as high mechanical stability. Good thermal isolation is thereby not only needed to minimize the overall power consumption but also to enable the integration of signal processing electronics in the same housing. Sufficient selectivity of metal oxide sensors can up to now only be achieved if the sensor is used in an application where the number of gases is limited such that cross-sensitivities can be neglected or if several sensors are put together to an array. In the latter case a lack of selectivity and therefore overlapping sensitivities of different sensors can be turned into an advantage [27]. Even though the use of array is promising with respect to sensor selectivity one has to keep in mind that the use of sensor arrays leads to an increased size of the sensor element or to the use several separate elements and thus to an increased power consumption. In the last few years the above mentioned difficulties have been overcome. The integration of gas sensitive metal oxide layer in microelectronic processing was achieved with the use of micromachining steps to yield micro-machined metal oxide gas sensors. This technology is promising to overcome the difficulties of screen-printed ceramic sensors due to the following facts.

Recent trends in application of metal-oxide gas sensors demands for thermal and mechanical performance such as low power consumption, fast response, and uniform temperature over the sensing layer and good mechanical stability at high temperatures [28-29]. For these objectives, the thermal characteristics of the microhotplate have to be well known and optimized, mainly with respect to power consumption, transient response and uniform temperature distribution, by controlling the heat losses, dielectric materials and heater configuration.[30-32] In the year 1997-98 Carole Rossi et. all experimentally proved that silicon base microheater using stalked dielectric membrane exhibit good performance with respect to power consumption [30-31]. In 2003 S. M. Lee et. all proposed some new designs for microheater which consumes very low power [33]. J. Puigcorbé at all in 2003 reported the development of a microheater for a metal oxide gas sensor and tested in order to characterize its thermal and mechanical behavior by combining experimental measurement with finite element method (FEM) simulation. Roy et.al.[34] in 2009

has already discussed elaborately the significance of co-planar structure with microheater and IDE produced by a single lithographic step on micromachined silicon substrates using a novel nickel alloy DilverP1 with its advantages over other heating elements.

Four different geometries single meander, double meander, fan type and square geometries are described by L. Sujatha et al. [35]. All four geometries are made of Poly-silicon material having same material properties and having 100um x 100um surface area. Also same voltages applied at ends to all geometries and can achieved maximum temperature of 483.83K. Among all four structures, square type geometry has cover vast area in which having more than 80% temperature. While Velmathi G et al. [36] describes the simulated results of micro-heaters having an improved temperature distribution over the sensing area and a higher density of integration is presented, by using six different patterns of micro-heater like Plane plate with central square hole, Double spiral, Honey comb, S- shape, fan shape and meander type with their Electro thermal simulated temperature profile. For the same supply voltage applied, the uniform temperature profile and the power consumption of the heater to get 400^{o}C is analyzed. High temperature uniformity is achieved in fan type patterns of micro-heater.

In 2001 S. Semancik et al. [37] introduced microhotplate platform made of poly-Si on the platform of SiO_2. They have used four arrow shaped electrodes for measuring heating temperature and observing change in sensing surface. Microhotplate is CMOS compatible and easily integrated on heterogeneous types of on chip circuits. In 2006 Bijoy kantha et al. [38] described implementation and fabrication process. They have made structure of Si_3N_4 layer on both side of silicon substrate. Also have SiO_2 insulating layer above Si_3N_4 layer and it has Ti/Pt micro-heater suspended on the top of the structure. They have used $BaSnO_3$ as sensing surface. Results are analyzed (resistance variation) at 600^{o} C and 700^{o} C for O_2 and CO gases. Velmathi G. et al. in 2010 has introduced six different geometries of micro-heater. They have used finite element method in COMSOL Multiphysics simulation tool. They have analyzed plane plate with central square hole, double spiral, honey comb, meander, fan type and s-type of geometries. Their 2D surface temperature is observed to achieve 400 ^{o}C temperature. Also resistive heating vs applied voltage characteristic was analyzed [39]. Jae-Cheol

Shim et al. describes the fabrication and characteristics of a NO sensor using ZnO thin film integrated SiC micro heater based on SiC thin film of operation in harsh environments. Sensitivity, response time, and operating properties in high temperature and voltages of NO sensors based SiC MEMS are measured and analyzed. As compare with only ZnO thin film, using the Pt added ZnO thin film was showed higher sensitivity, lower working temperature, and faster adsorption characteristics to NO gas than the pure ZnO thin film [40].

2.2 Objectives

The main objectives of presented work are as follows:

1. To describe and simulate different micro-heater geometries using COMSOL Multiphysics and to analyze which geometry gives better temperature uniformity.
2. To achieve a geometry optimization in fixed surface area for given structure for temperature uniformity.
3. To put a sensing layer on the heater surface and analyze the effect of presence of a gas through interdigitated transducer (IDT).
4. Use IDT to analyze the resistivity change of the sensing layer due to presence of gas.

2.3 Thesis organization

Chapter 3 covers the research methodology used in this project. Finite Element Analysis (FEA) package of COMSOL Multiphysics is used for design and simulation of micro- heater geometries of metal oxide based gas sensor. Joule heating and thermal expansion physics of structural mechanics module is used to generate micro-heater geometries. Computer simulation has certain advantages because it provides design optimization by changing materials of the device, its properties, geometries and layer dimensions without actual fabrication.

Chapter 4 describes the design parameters of metal oxide gas sensor. It explain the design parameters of micro-heater and effect of this parameter on sensing surface of MEMS based metal oxide gas sensors. It also explains different micro-heater geometries comparison for gas sensor and best shape is selected among all

the choice for improving temperature uniformity in gas sensor for proper detection of gases.

Chapter 5 gives shape optimization of selected micro-heater geometry to enhance better temperature uniformity. It gives relation between maximum surface temperature with applied voltage. The microheater is integrated with coplanar IDT above which is a sensing layer.

Chapter 6 describes the fabrication steps to design micro-heater for MEMS based gas sensor. This will helpful to fabricate MEMS based gas sensor with Poly-Si and/Platinum based micro-heater.

Chapter 7 concludes this project after all results compared in Chapter 5. Also it gives idea about future work possible in this field.

CHAPTER-3

INTRODUCTION TO COMSOL

3.1 COMSOL Multiphysics: An Introduction

It provides Finite Element Analysis (FEA), solver, simulation. It has packages for engineering and general physics applications based on advanced numerical method so it is generally called as "Multiphysics". In early year, this software was known as "FEMLAB". The basic idea of this tool is to mimic as similarly as possible the effects that are noticed in real world. This tool also offers to add coupled system of PDE (Partial Differential Equations). It provides simulation platform along with their dedicated physics tools for AC/DC module, electrical, chemical, plasma, general physics etc.

With the help of built in interfaces and modern support for defining material properties, it is very easy to make models implementing the suitable physical quantities such as, constraint, supply sources, fluxes (electrical or heat) , its material properties without specifying the underlying equations [41]. User can define their own expressions, variables. COMSOL basic window is shown in Fig. 3.1.

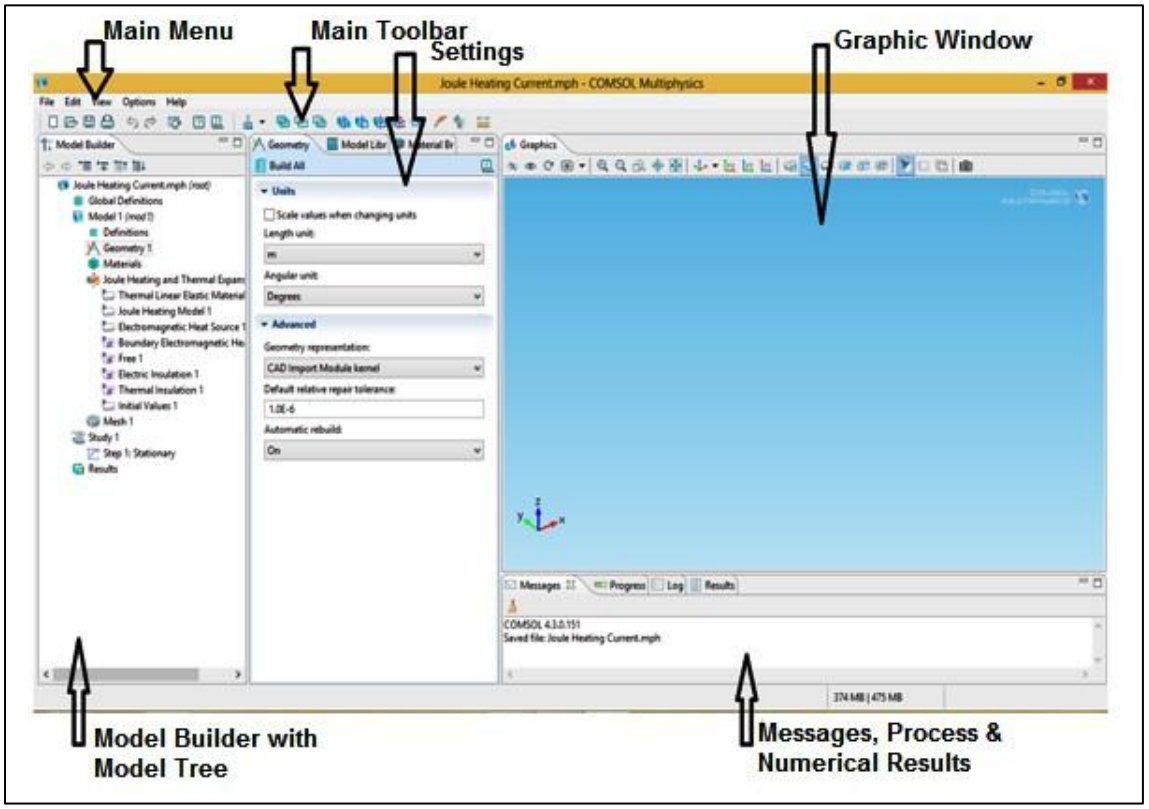

Fig. 3.1 COMSOL Multiphysics window.

User has to add physics with specific sub-physics (Specific area of simulation or specific operation of that physics). Also user has to define study type for analysis. Study types options are mentioned below:

- Preset Studies
  - Eigen Frequency
  - Stationary
  - Time Dependent
- Custom Studies
  - Empty Study
  - Eigen Value
  - Frequency Domain

One can change/add study during simulation process also. There are many available choices like, parametric sweep response, cluster computing etc. Fig 3.2 shows setup study tab on simulation window.

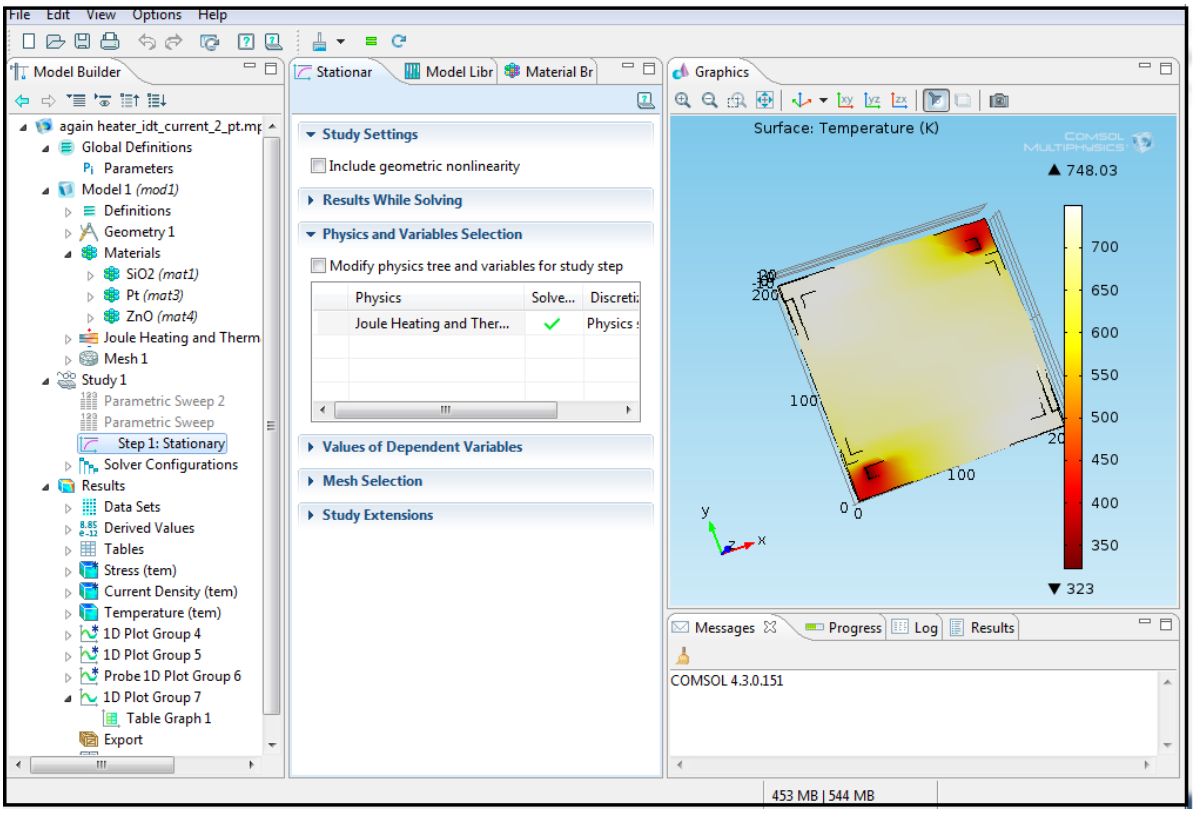

Fig. 3.2 Setup study type in COMSOL Multiphysics

COMSOL Multiphysics supports many applications area. It also provides some live link module such as with MATLAB, CAD and Excel.

All the application modules are mentioned in the list:

- AC/DC Module
- Acoustics Module
- Batteries & Fuel Cells Module
- CAD Import Module
- CFD Module
- Chemical Reaction Engineering Module
- Corrosion Module
- ECAD Import Module
- Electrochemistry Module
- Electrodeposition Module
- Fatigue Module
- Geomechanics Module
- Heat Transfer Module
- LiveLink Products for CAD
- LiveLink for MATLAB
- LiveLink for Excel
- Material Library
- MEMS Module
- Mixer Module
- Microfluidics Module
- Molecular Flow Module
- Multibody Dynamics Module
- Nonlinear Structural Materials Module
- Optimization Module
- Particle Tracing Module
- Pipe Flow Module
- Plasma Module
- RF Module
- Semiconductor Module
- Structural Mechanics Module

- Subsurface Flow Module
- Wave Optics Module

3.2 Joule Heating and Thermal Expansion Interface

The Joule heating and thermal expansion interface (Physics) is found under the **Structural Mechanics** branch in the **model wizard window.** It has combination of Heat transfer interface, electric current interface and also Structural Mechanics interface.

The Joule Heating Interface

The Joule Heating physics is combination of two different modules: electric current interface which is part of AC/DC module and Heat transfer interface. Joule heating is also called as resistive heating or ohmic heating.

As mentioned earlier, there is interaction of both modules, which may occur in both directions:

1. In the Electromagnetic Heat Source node, this resistive heating is visible as a heat source.
2. To use default setting value for electric conductivity from the material. From the choice from Conduction current→ Electrical Conductivity list, and choose the Linearized resistivity which is basically temperature dependent and described by the following equation.

$$\rho = \frac{\rho_0}{\left(1+\alpha\left(T-T_0\right)\right)} \qquad (3.1)$$

Where α is the temperature coefficient of resistivity, which describes how the resistivity varies with temperature and ρ_0 is the resistivity at reference temperature T_0.

The dependent variables may be temperature T and electric voltage potential V. Joule Heating and Thermal Expansion physics is selected and parameters are defined for the structure under analysis which is shown in Fig. 3.3. They are interface parameters; we can add more parameter as per our requirements of parameter definition by simply right clicking on Joule Heating and Thermal Expansion physics. Generally we add parameter definition like, Fixed constraint from Structural Mechanics, Ground and Electric Potential from Electric Current, Temperature and Heat Flux from Heat Transfer physics

defined under main module.

They are defined like [42],

- Thermal Linear Elastic Material
- Joule Heating Model
- Electromagnetic Heat Source
- Boundary Electromagnetic Heat Source
- Free
- Electric Insulation
- Thermal Insulation
- Initial values
- Terminal
- Ground
- Heat Flux
- Temperature
- Fixed Constraint

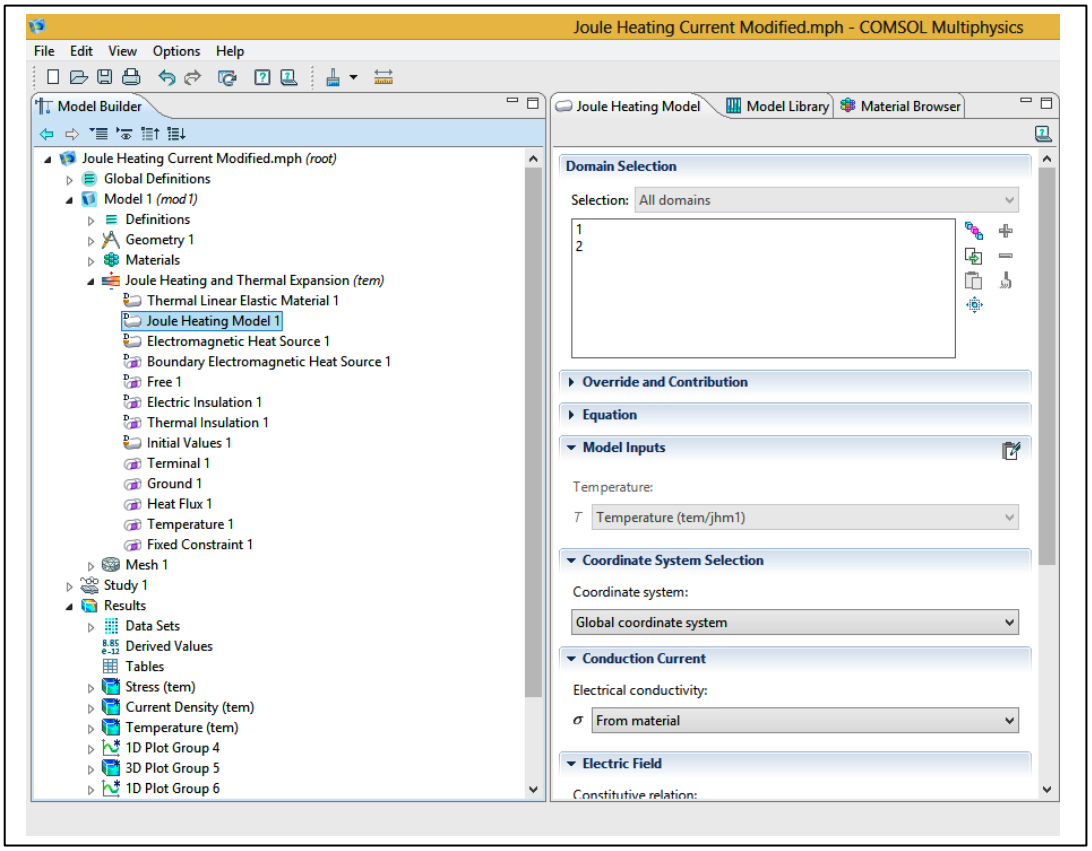

Fig. 3.3 Joule Heating and Thermal Expansion module window in COMSOL Multiphysics

3.3 Electro – Thermal Mathematical Modeling in Joule Heating

Joule Heating model contains the following important sections:

Domains

While analyzing any structure, one should select the domain on which he/she wants to apply Joule Heating and Thermal Expansion model, otherwise it select all domain by default [43].

Dependent Variables

The Joule Heating Model node in COMSOL uses the following version of the heat equation as the mathematical model for heat transfer in solids:

$$\rho C_p(\partial T/\partial t) - \Delta(k\Delta T) = Q \qquad (3.2)$$

With the following material properties:

- $\boldsymbol{\rho}$ is the **density**.
- $\boldsymbol{C_p}$ is the **heat capacity.**
- $\boldsymbol{k}$ is the **thermal conductivity** (a scalar or a tensor if the thermal conductivity is anisotropic).
- **Q** is the **heat source** (or sink).

For Joule heating, it comes from the electric current and is added in the Electromagnetic Heat Source node. For a steady-state condition, obviously temperature does not vary with time so we can eliminate first term. In addition, an electric current equation is also added in analysis.

When an electric current flows in a solid or in liquid having finite conductivity, it converts electric energy into heat through material resistive losses which is widely known as joule heating. Resistive heat generated Q is proportional to square of current density J . Electric field E is equal to negative of gradient of voltage potential V. Also there is proportional relation between current density J and electric field E and there is reciprocal relation between conductivity ' σ' which is function of temperature and a resistivity ' ρ'.

From the above discussion,

$$Q \propto |J|^2 \tag{3.3}$$

$$\sigma = \sigma(T) \tag{3.4}$$

$$\rho = \frac{1}{\sigma} \tag{3.5}$$

$$O = \rho \cdot |J|^2 = \frac{1}{\sigma}|\sigma \cdot E|^2 = \sigma \cdot |\nabla V|^2 \tag{3.6}$$

For particular temperature range, the electric conductivity σ is a function of temperature T given by,

$$\sigma = \frac{\sigma_0}{1+\alpha\left(T - T_0\right)} \tag{3.7}$$

Where α is the temperature coefficient of resistivity, which describes how the resistivity varies with temperature and σ_0 is the conductivity at the reference temperature T_0. Also power consumption is describe as,

$$P = \frac{V^2}{R} \tag{3.8}$$

Where V is electric potential applied and R is resistance of heating electrode. As explained in (3.8), power consumption is directly proportional with square of applied voltage and also inversely proportional with the resistance of used material.

The equations have been solved and simulation is done under Dirichlet, Neumann, and mixed boundary conditions using the Finite Element Analysis (FEA) method when the Electro-Thermal module is selected in COMSOL Multiphysics. Also for simulation purpose, fixed applied electrical potential and fixed temperature and the ends of the material terminal is considered.

3.4 Model Inputs

This section contains values and fields, which are considered as inputs to expressions that define material property. If you have added such user defined property groups, their model inputs appears here. Initially, it is empty section.

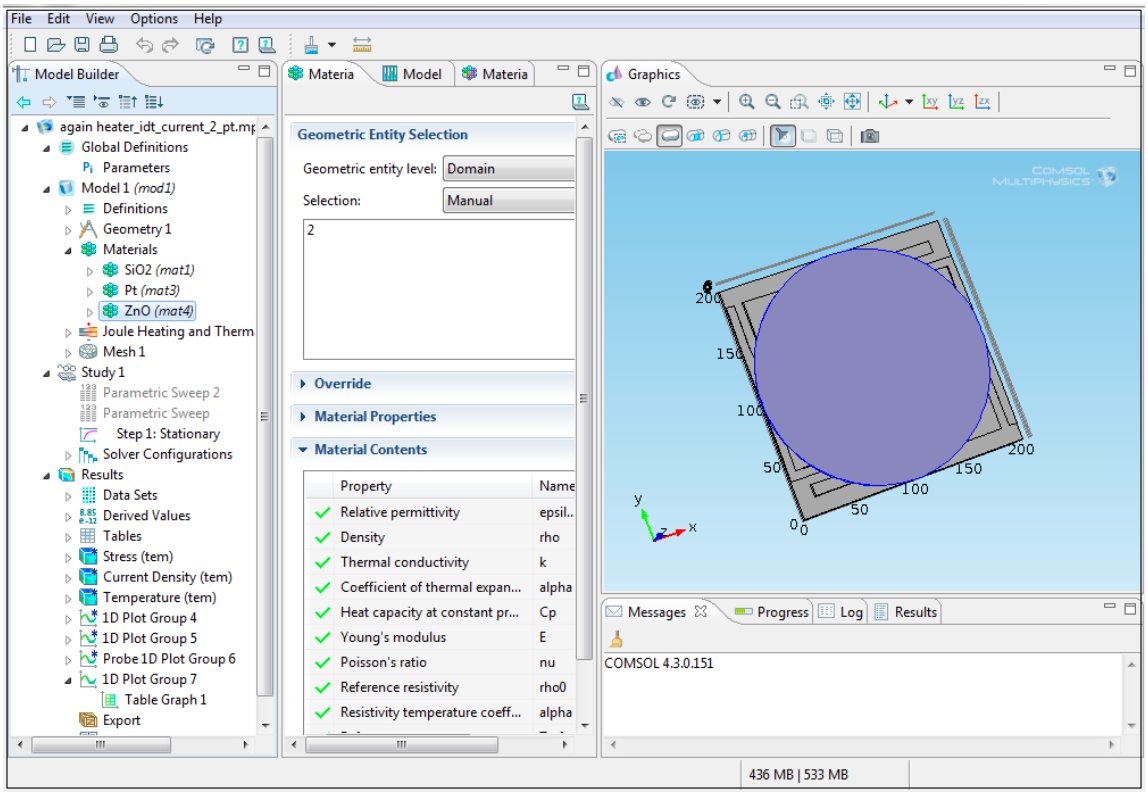

Fig. 3.4 Material Selection in COMSOL Multiphysics 4.3

Conduction Current

It has SI unit of S/m and it defines electrical conductivity. We have already discussed this in previous section. User have to go to Joule Heating and Thermal Expansion Model→ Joule Heating Model → locate Conduction Current → Electrical Conductivity and have to change it from user defined to Linearized resistivity.

Heat Conduction

There is default setting to use the thermal conductivity from the material. If anyone wants to give his/her own value, select option of user defined. It has SI unit as [W/(m.K)]. The thermal conductivity k gives relation between the temperature gradient ΔT and the heat flux vector q. Path will be Joule Heating and Thermal Expansion Model → Joule Heating Model → locate Heat Conduction → choose

option as from material.

Electromagnetic Heat Source

The Electromagnetic Heat Source feature is only available in the Joule Heating predefined COMSOL Multiphysics interface. It is added as default node. Joule heating is proportional to I^2R, where I is electric current and R is resistance of material.

Initial Values

The initial Values node adds initial values for the temperature T and the electric potential V that can serve as an initial condition for a transient simulation or as an initial guess for a non linear solver. If users need to specify more than one set of initial values, then one can add addition Initial Values features. Generally, temperature is taken as room temperature (293.15 K) and electric voltage potential is 0V.

Free

Free feature is considered as default boundary condition. That means that there is no loads and/or no constraint acting on boundary. In micro-heater, this feature is used for edge.

Ground

This feature is not given directly but we have to choose by right click on Joule Heating and Thermal Expansion Model and choose electric currents then choose ground option. In micro-heater, we have to define one end as electric potential and other as ground.

Fixed Constraint

We have to make fix structure sometimes domain or edges or boundary to withstand against stress and joule heating. It may change structure. So there is one option available by right clicking Joule Heating and Thermal Expansion Model →Structural Mechanics → Fixed Constraint.

3.5 Conclusion

In this chapter, we have studied and discussed about the COMSOL Multiphysics simulation tool with its features and different modules. As we will design and simulate different micro-heater geometries, this module will helpful to analyzing results and understand the behavior of micro-heater with respect to its properties.

CHAPTER-4

MICROHEATER DESIGN

4.1 INTRODUCTION

In most cases microheater must be a small structure fabricated using a CMOS-compatible process with a good fabrication yield and having the lowest possible power consumption. Microheaters consist generally of a hot plate on a membrane micro machined from bulk silicon. The temperature rise is obtained by the Joules heating in a resistor deposited on a membrane a few micrometers thick. The material commonly used for the substrate is Si because of its excellent mechanical properties. Another advantage of using Si is that the electronics circuits and the sensor can be integrated on one single chip.

4.2 Micro-heater

MEMS Micro-heaters can generate high temperature at low power and also exhibit fast response time. Generally micro-heaters have a thin film heater coil or wire which may be suspended within silicon for better thermal isolation. Usually, micro-heaters have platform of Silicon dioxide (SiO_2) or Silicon Nitride (SiN_4). They are capable to operate at temperatures up to 600^o C.

The power consumption or heating power (P) can be calculated using formula as explained below:

$$P = \frac{V^2}{R} \tag{4.1}$$

Where V is an applied voltage and R is a resistance across two ends of micro-heater. The value of resistance can be found by mentioned formula for given micro- heater geometry:

$$R = \rho \frac{l}{w \cdot h} \tag{4.2}$$

Where ρ the value of resistivity of material, *l* is the length, *w* is the width and *h* is the height of micro-heater.

A structure of micro-heater is shown in Fig. 4.1, where 200 x 200 μm^2 platform of Silicon dioxide (SiO_2) is used and above it micro-heater is placed.

4.3 Micro-heater Design issues

The micro-heater design is essential to restrain the temperature distribution and also to reduce power consumption. To fulfill a desired temperature distribution, user has to choose proper micro-heater geometry and substrate.

Some of the basic requirements must keep in mind those are as follow:

- Material used
- Uniform temperature distribution over the heater
- Mechanical stability
- Long life
- Micro-heater geometries
- Low power consumption

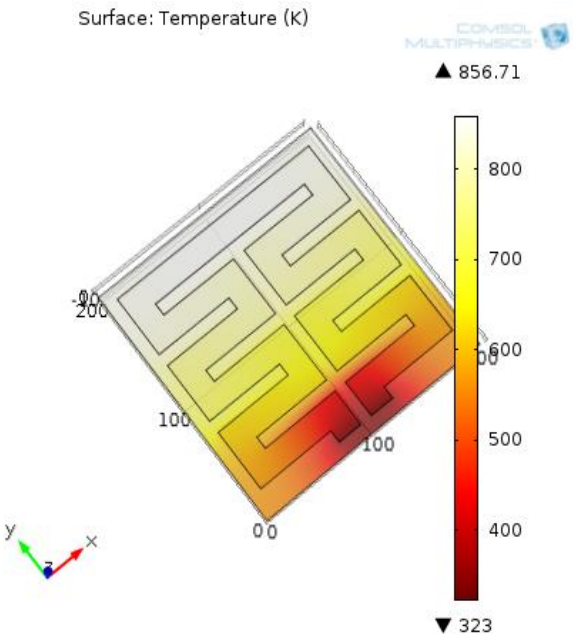

Fig 4.1 A structure of micro-heater.

Material used: For most effective performance, it is a primary necessity to choose an ideal material for micro-heater. Mostly, the value of resistivity of material used micro-heater should be high. Platinum (Pt), Gallium nitride (GaN), Gallium arsenide (GaAs), Titanium nitride (TiN), DilverP1 (alloy of Ni, Co, Fe), Poly silicon (Poly-Si) and many metal alloys etc. are widely used materials for micro-heater [47].

Uniform temperature distribution over the heater: It is essential need of micro-heater to have better temperature uniformity for proper detection of desired gases [26]. So choice of micro-heater geometry which can distribute temperature equally throughout the sensing surface area without generating any "hot spot" is desirable.

Mechanical stability*:* For having long life and mechanical stability of micro-heater, we should minimize stress and displacement. This is totally dependent on micro-heater material and its geometry. Also the deformation gradient and thermal expansion of micro-heater must be lower that will helpful to achieve better results.

Long life: Micro-heater geometries plays a vital role for achieve better temperature uniformity. There are many micro-heater geometries are available and are to investigated and simulated to attain uniformity.

Micro-heater geometries: While choosing micro-heater thickness, one should care about material strength and heat consumption of the geometry to avoid more heat dissipation loss. Preferred materials used as membrane under microheater for heat (thermal) isolation are Silicon dioxide (SiO_2) and Silicon nitride (Si_3N_4), though Si_3N_4 is having more heat consumption than SiO_2 [31].

Low power consumption: Low power consumption is most important parameter among all especially for battery operated sensors. As we have already seen the power consumption equation, by decreasing width and height of micro-heater geometry, we can increase resistance and that causes reduction in overall power consumption. So dimensions of micro-heater are very critical for making low power gas sensor.

4.4 Advantages of Coplanar Microheater

Both the microheater and the interdigitated electrode are placed laterally on the same insulating substrate. Because of the high thermal conductivity of silicon membrane there is no need of the stacked structure. Rather microelectrodes can be placed on the same layer at an optimum distance from the microheater leading to a novel coplanar design.

The advantages of this coplanar heater are:

(a) Fast response time

(b) Better temperature uniformity over the membrane area

(c) Ease of fabrication

4.5 Selection of micro-heater material

To find micro-heater material, it is necessary to discuss material parameters such as thermal conductivity, coefficient of thermal expansion and thermal conductivity. Cooling time or heating time of micro-heater actually depends on thermal conductivity. More the value of thermal conductivity of material, higher will be the value of rise time. Also cooling time is always marginally higher than rise time. This difference is clearly seen in metals. Variation in object size with temperature change is dependent on coefficient of thermal expansion. This is measurement of fractional change in size of structure per degree change in temperature at constant value of pressure. Lastly, electrical conductivity represents how the temperature increases due to joule heating.

It has always been a challenge to select proper material for micro-heater to achieve desired temperature requirement for any gas sensor. We have already discussed various materials available for micro-heater like, Titanium nitride (TiN), Gallium nitride (GaN), Gallium arsenide (GaAs), DilverP1 (alloy of Ni, Co, Fe), Poly silicon (Poly-Si), Platinum (Pt) and many metal alloys like brass and alnico [47]. Among them Titanium nitride (TiN), Gallium nitride (GaN), Gallium arsenide (GaAs) are less preffered materials as they have certain major disadvantages. Dilver P1 has many advantages such as high yield stress, low thermal power thermal expansion, low thermal conductivity.

Here we have used Platinum (Pt) as a material for micro-heater since, Platinum (Pt) has very high temperature stability (because melting point is high) so it can easily withstand at very high temperature. Also it can attain high temperature by applying very small voltage.

4.6 Micro-heater geometries and their simulation results

Various types of micro-heater geometries are simulated and analyzed using simulation tool COMSOL Multiphysics 4.3 to achieve basic two requirements namely, high temperature uniformity and low power consumptions.

For the simulation purpose, all geometries are made of Pt with micro-heater geometry height of 2 µm and with 200 x 200 μm^2 surface area with platform of SiO_2 to provide thermal insulation to improve temperature profile [48]. Also in micro-heater geometries, one end of micro-heater is having applied voltage of 1.0 V and the other end is grounded. Comparison has been made for three most desired micro-heater geometries as mentioned below.

- Single meander
- Double meander
- S-shape

The purpose of simulation of above geometries is to find the best suitable geometry which proves better temperature uniformity, so surface temperature will not be under consideration. Every simulation result represents temperature distribution by rainbow colors. Where red color area represents maximum temperature and blue area represents minimum temperature (minimum temperature is defined during boundary conditions).

1) Single meander

Single meander geometry is simulated and result of surface temperature distribution is shown in Fig. 4.2. Simulation result displays very less temperature uniformity.

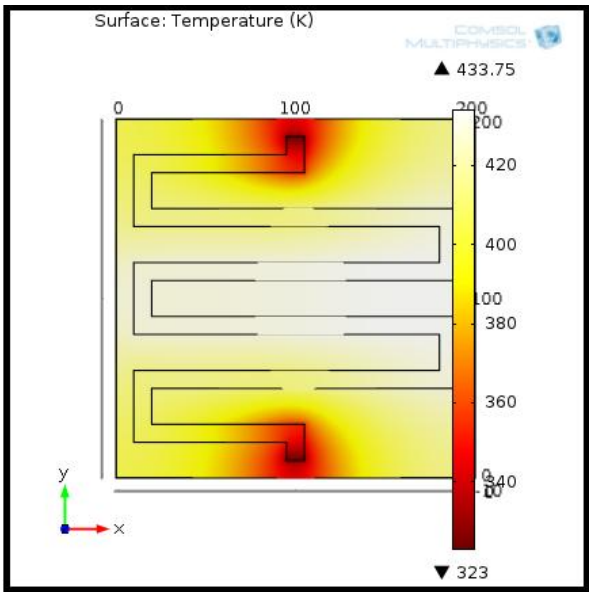

Fig. 4.2 Temperature profile of Single meander microheater.

2) Double Meander

Single meander and double meander geometry are most studied and researched geometries among all as they are easy to design and fabricate [39]. Fig 4.3 demonstrates the double meander geometry with its simulation result of temperature distribution. There is a vast improvement in temperature uniformity as compared to single meander geometry.

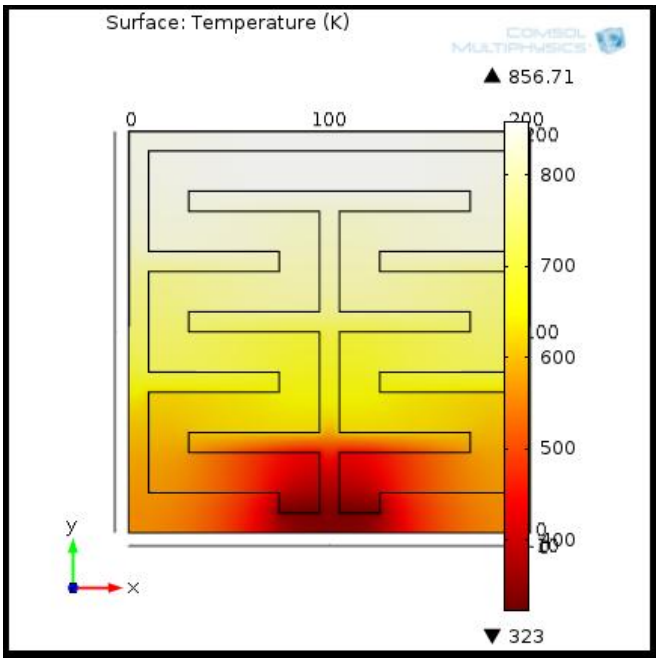

Fig. 4.3 Temperature profile of double meander microheater.

3) S-shape Microheater

Fig. 4.4 shows simulation result of S-shape geometry where it can be observed that it has greater uniformity. Heater was made of Pt on an insulating base.

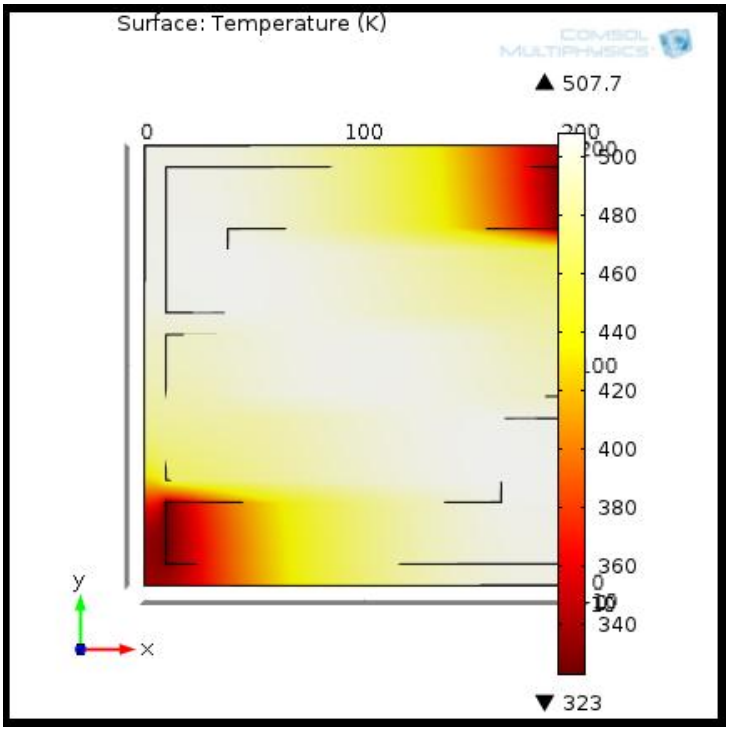

Fig. 4.4 Temperature profile of s-shape microheater.

4.7 Conclusion

We have simulated various micro-heater geometries but S-shape and double meander geometries provides better temperature uniformity. S-shape geometry has high stress and less stability at high temperature as more deposition in middle portion of geometry. In the next chapter, we will simulate this s-shape micro-heater geometry by using Platinum as micro-heater material. There will be discussion on width variation of micro-heater geometry and its effect on temperature uniformity. All results will be compared and conclusion will be made based on these results.

CHAPTER-5

RESULTS AND DISCUSSION

5.1 Parameters consideration under electro – thermal analysis

During the simulation and result analysis, some parameters of micro-heater are considered as most crucial as they directly affect the performance of gas sensor. They are mentioned below:

- Maximum temperature
- Temperature uniformity
- Power consumption
- Transient temperature response
- Transient resistance response of micro-heater
- Current density

We have already discussed parameters like, maximum temperature, temperature uniformity and power consumption so they are not deliberated further in discussion. As response/recovery time of gas sensor is dependent on sensing surface temperature and sensing surface temperature is relied on transient temperature response of micro-heater, it is more crucial to have minimum transient temperature response time of micro-heater. Due to joule-heating there is variation in resistance of micro-heater. As temperature increases, value of resistance raises. Also current density represents the distribution of current on the micro-heater surface (current / area).

5.2 Electro-Thermal analysis

In the previous chapter, various geometries are tried and analyzed for optimum solution of micro-heater geometry. Then modified spiral geometry is found as optimum solution which having high resistance value (which is helpful for resistive heating) and less power consumption. We have already discussed resistive heating (Q) equation in previous chapter i.e,

$$Q = \sigma \cdot |\nabla V|^2 \tag{5.1}$$

For particular temperature range, the electric conductivity σ is a function of temperature T given by:

$$\sigma = \frac{\sigma_0}{1+\alpha\left(T - T_0\right)} \tag{5.2}$$

Where α is the temperature coefficient of resistivity.

The basic resistance equation including cross sectional area A is given by:

$$R = \frac{\rho \cdot l}{A}$$
$$= \frac{l}{\sigma \cdot A} \tag{5.3}$$

From above equation it is clear that, electric conductivity σ and cross sectional area A are inversely proportional. Also from equation (1), we can conclude that either increases the voltage gradient of micro-heater two ends (simply increases applied voltage potential of electrode) or increases the area (thickness or width) of micro-heater. Let us discuss two cases in which variations in voltage gradient and variations in thickness / area (thickness * width = area) of micro-heater geometry is analyzed for measure changes in temperature and power consumption of micro-heater.

5.3 Design of S-shape Microheater Geometry

S-shape geometry which is shown in Fig. 5.3.1, is having 2 µm thickness and it is placed on 200 x 200 μm^2 insulating platform of SiO_2 having 3 µm thickness. All dimensions are shown in Fig. 5.3.2. Properties of SiO_2 and Pt are defined in **Appendix 1**. As shown in Fig. 5.3.2, micro- heater has equal stripe width of 20 µm throughout.

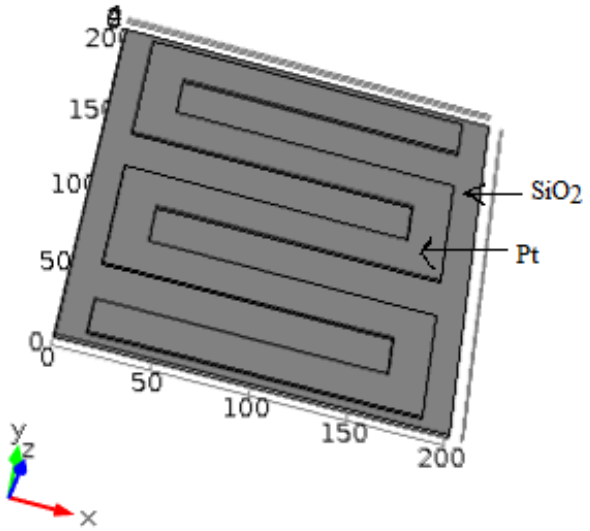

Fig. 5.3.1 3D view of Pt based S-shape geometry.

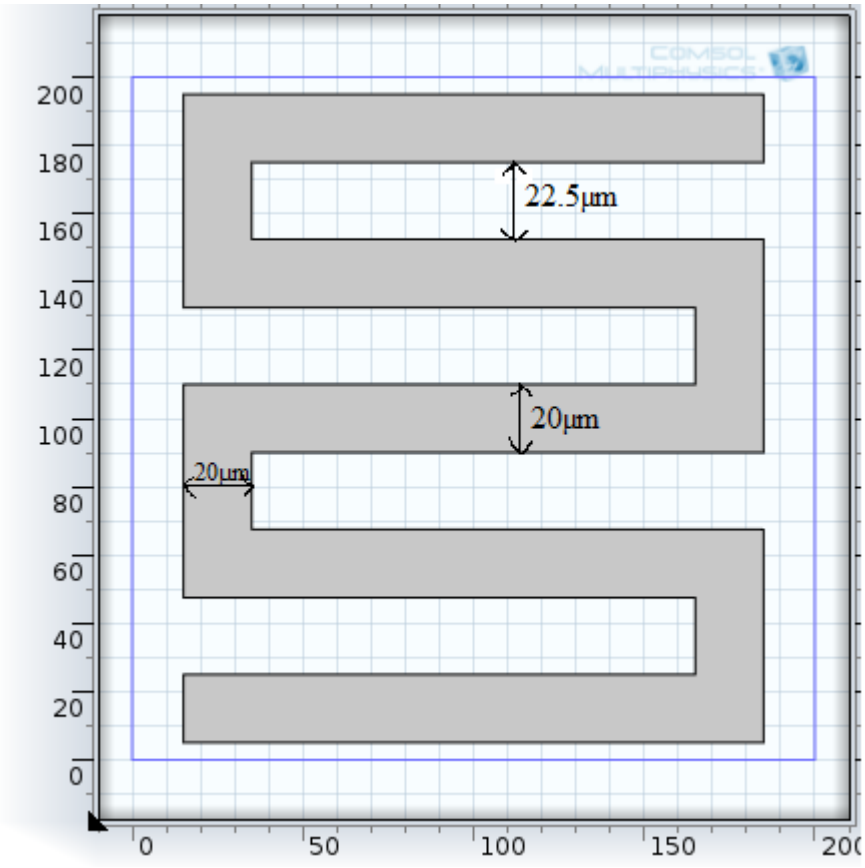

Fig. 5.3.2 2D view of S-shape geometry with dimensions.

Next goal is to place the IDT co-planar to the microheater. IDT is used to detect the changes in the sensing layer in presence of a gas. Fig. 5.3.3 shows placement of the two interdigitated electrodes (IDE's) with respect to the microheater on the same insulating base. The red color shows the IDE's. The IDE's are also made of Pt and have same stripe width of 7 µm throughout. Fig. 5.3.4 shows the dimensions of the IDE's.

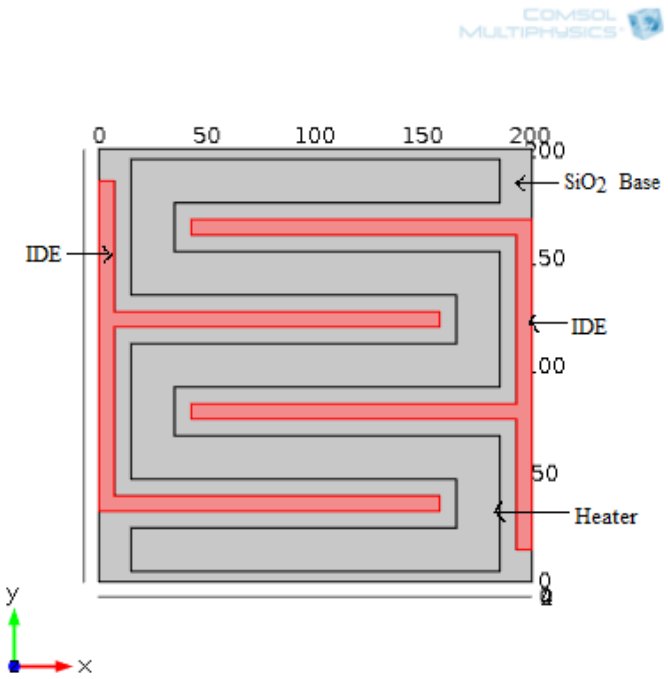

Fig. 5.3.3 IDT placed coplanar to microheater.

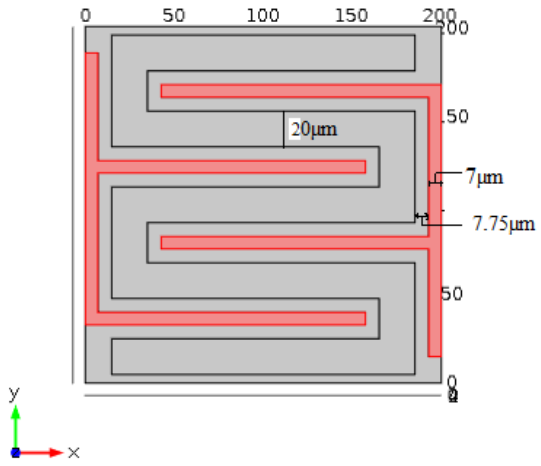

Fig. 5.3.4 Dimensions of IDT placed coplanar to microheater.

A gas sensitive layer of ZnO is used for gas sensing purpose. Whenever there is a ambient gas present in the atmosphere it will react with the sensing layer in presence of heat provided by the microheater. So a circular shape sensing layer is placed over the surface of microheater as shown in Fig. 5.3.5. The sensing layer has a thickness of 2 µm.

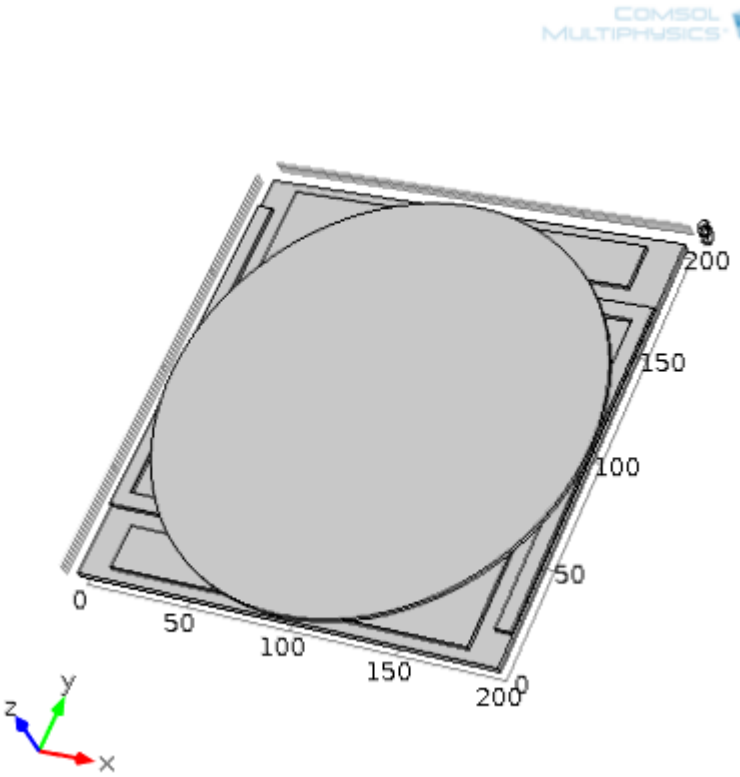

Fig. 5.3.5 3D view of the microheater and IDT over which the sensing layer is deposited.

5.4 Simulation Results of S-shape Microheater with IDT and Sensing Layer

Now apply a voltage of 0.5V across the terminals of the microheater to obtain the necessary temperature. The base of SiO_2 which is 3 µm thick will provide an insulation path for the heat to protect the device from any damage. Fig. 5.4.1 shows the temperature distribution across the geometry.

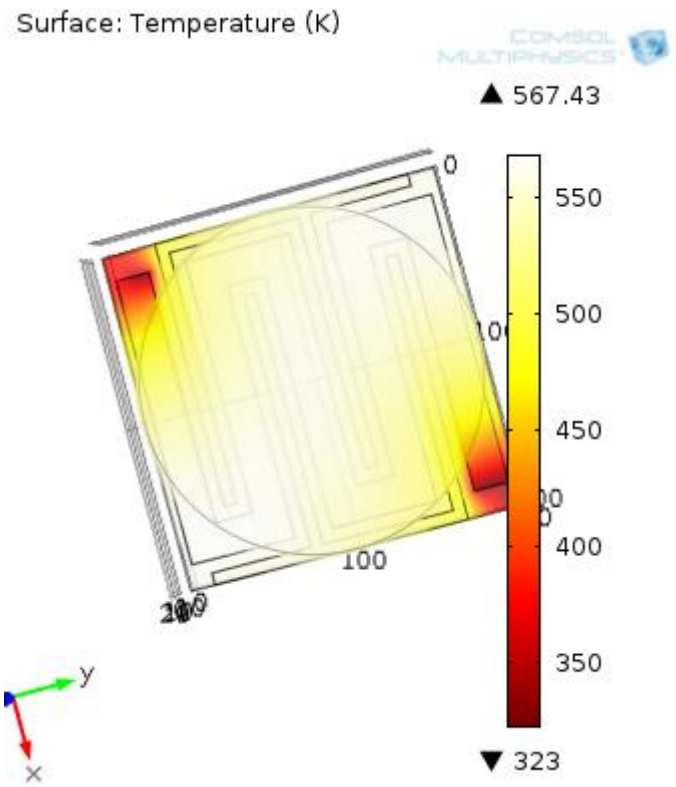

Fig.5.4.1 Temperature distribution over the uniform width S-shape microheater.

To obtain better temperature uniformity we have to choose a varying width microheater.

Changing the width of microheater will help in providing more uniformity. Fig. 5.4.2 shows the geometry of varying width S-shape microheater. It has a width of 10 µm on the top and bottom edges and 20 µm width in the rest of the region.

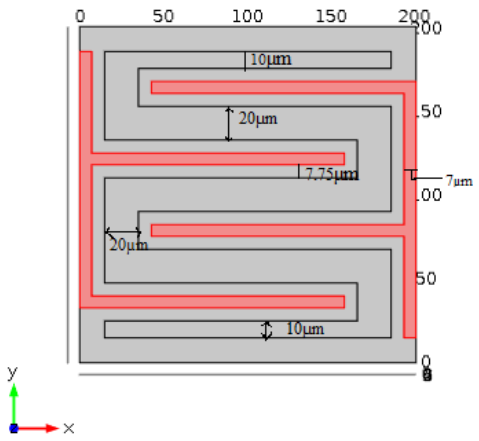

Fig. 5.4.2 2D view of varying width S-shape microheater with coplanar IDT.

5.4.1 Simulation result of varying width S-shape microheater:

For the s-shape heater we designed we apply a voltage of 0.5V across the terminals of the microheater to obtain the necessary temperature. The base of SiO_2 which is 3 µm thick will provide an insulation path for the heat to protect the device from any damage. Fig. 5.4.3 shows the temperature distribution across the geometry.

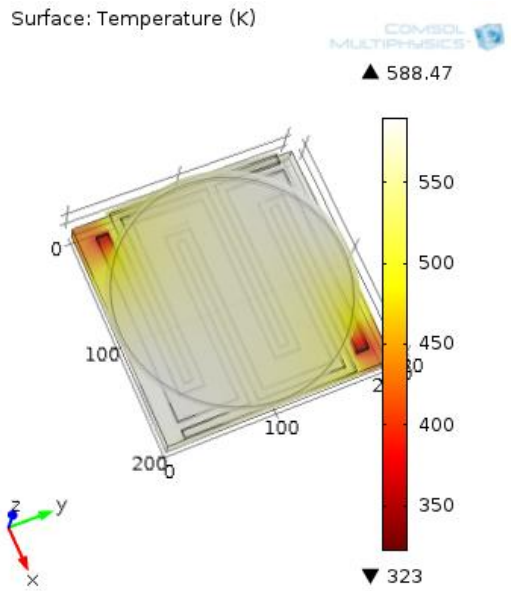

Fig. 5.4.3 Temperature distribution for varying width S-shape microheater.

Comparing Fig. 5.4.1 and Fig. 5.4.3 it can be easily observed that the varying width microheater provides better temperature uniformity than the uniform width microheater. This geometry is used for further research.

A graph of temperature variation for both the above geometries is shown in Fig. 5.4.4. It shows the temperature distribution along the line joining the two terminals of the heater (y=x) for the s-shaped microheater. In this figure the solid black line shows the temperature variation for uniform width s-shape heater and the green dashed line for non-uniform width heater. From Fig.5.4.4 it can be analyzed that better temperature uniformity is obtained in case of non-uniform width heater.

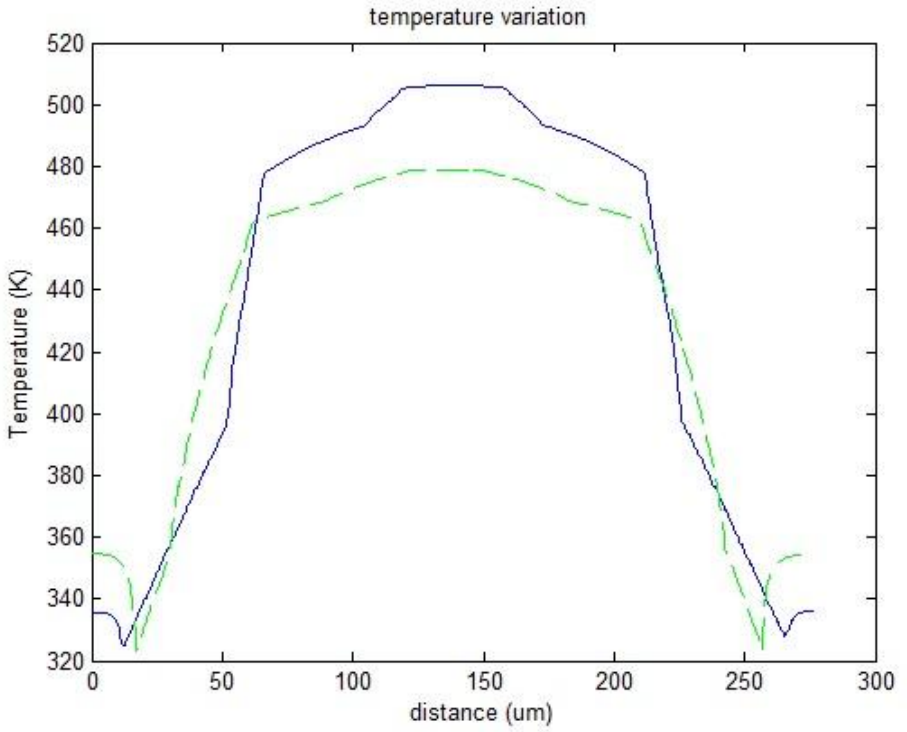

Fig.5.4.4 Temperature variation along the line between two terminals of s-shape microheater.

5.5 Design of Double Meander Shaped Microheater Geometry

Double meander geometry having 2 µm thickness is shown in Fig. 5.5.1, and it is placed on 200 x 200 μm^2 insulating platform of 3 µm thick SiO_2. For the insulating platform SiO_2 is used as a material and for microheater Platinum is used. All dimensions are shown in Fig. 5.5.1. Properties of SiO_2 and Pt are defined in **Appendix 1**. As shown in Fig. 5.5.1, micro- heater has equal stripe width of 20 µm throughout.

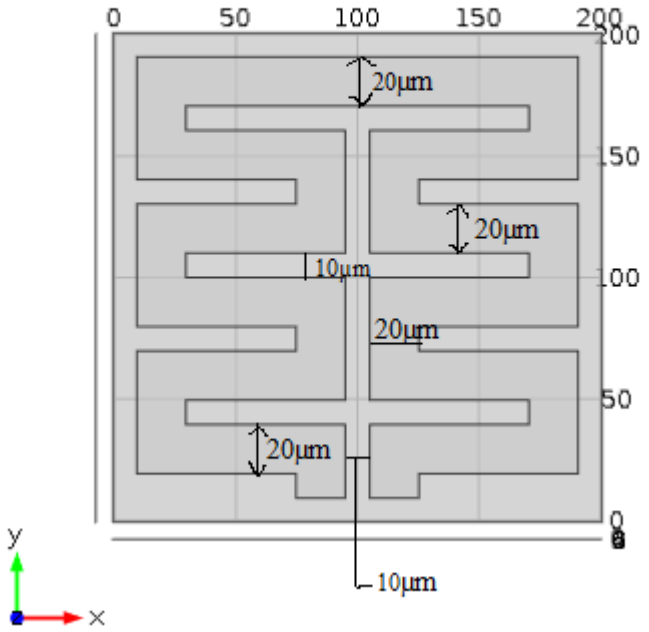

Fig. 5.5.1 2D view of double meander geometry with uniform width.

5.5.1 Simulation result for double meander shape microheater

A voltage of 0.5V is applied across the terminals of the microheater to generate the necessary heat required by the gas sensor. Fig. 5.5.2 shows the simulation result for the uniform width microheater over which sensing layer of ZnO is also presented.

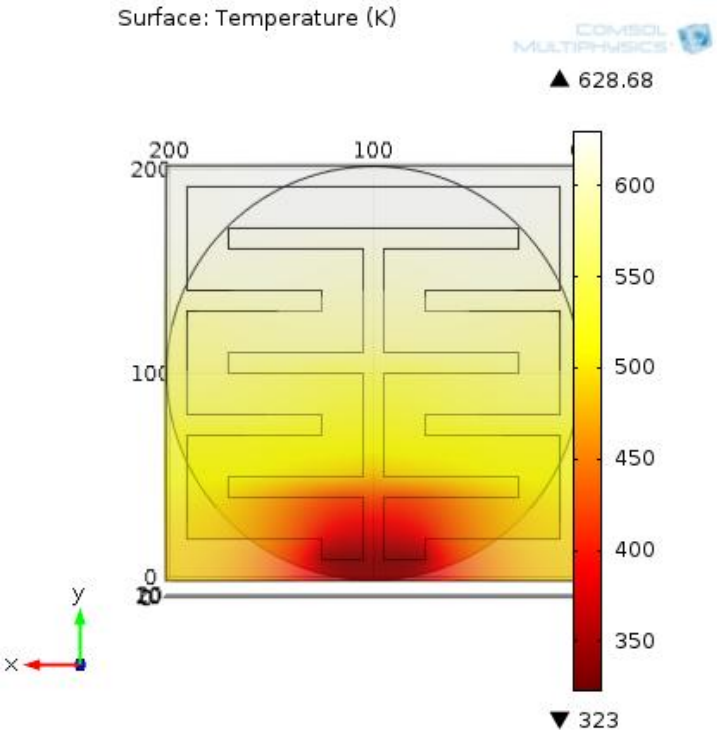

Fig. 5.5.2 Temperature profile for uniform width double meander microheater.

To improve the temperature uniformity a varying width double meander shape microheater is used, as shown in Fig. 5.5.3.

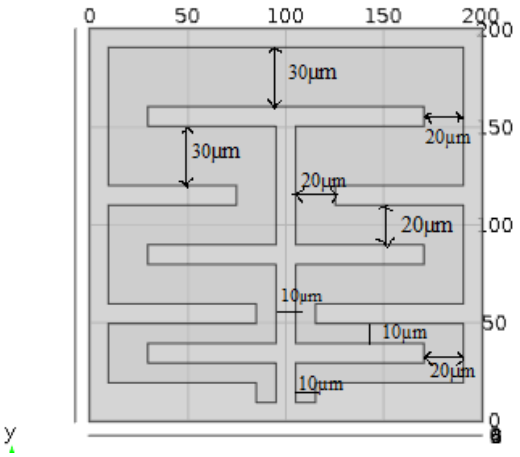

Fig. 5.5.3 Dimensions of modified varying width double meander microheater.

Simulation result for varying width double meander microheater when supplied a voltage of 0.5V across the microheater terminals is shown in Fig. 5.5.4. This figure also includes the sensing layer.

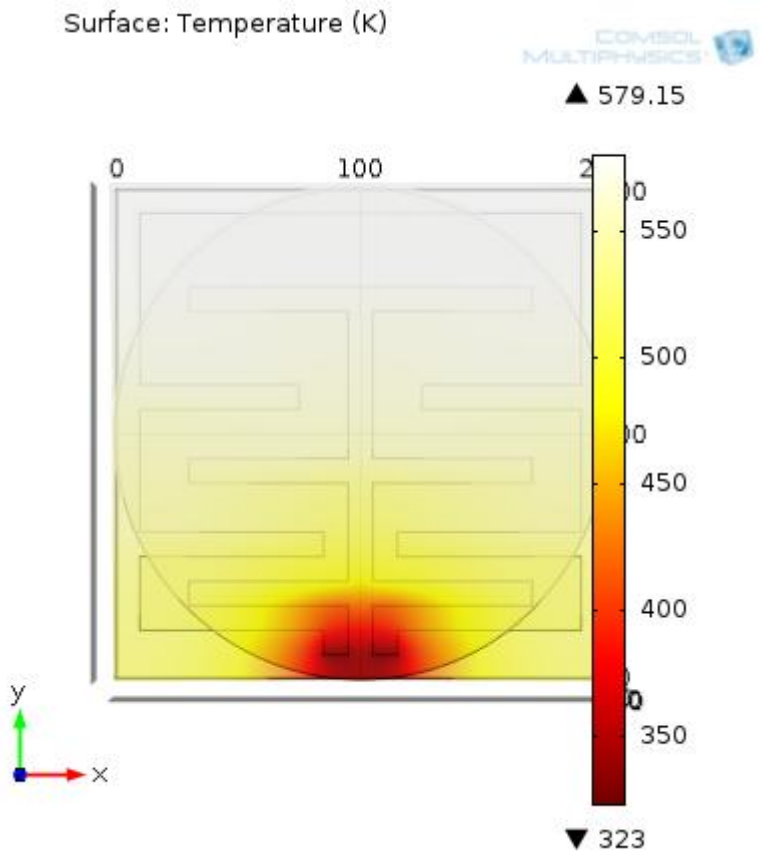

Fig. 5.5.4 Temperature profile for varying width double meander microheater.

A graph of temperature variation for both the above geometries is shown in Fig. 5.5.5. It shows the temperature distribution along the line (x= 100μm) between the two terminals of the heater for the double meander type microheater. In this figure, the solid black line shows the temperature variation for uniform width heater and the green dashed line for non-uniform width heater. From Fig.5.5.5 it can be analyzed that better temperature uniformity is obtained in case of non-uniform width heater.

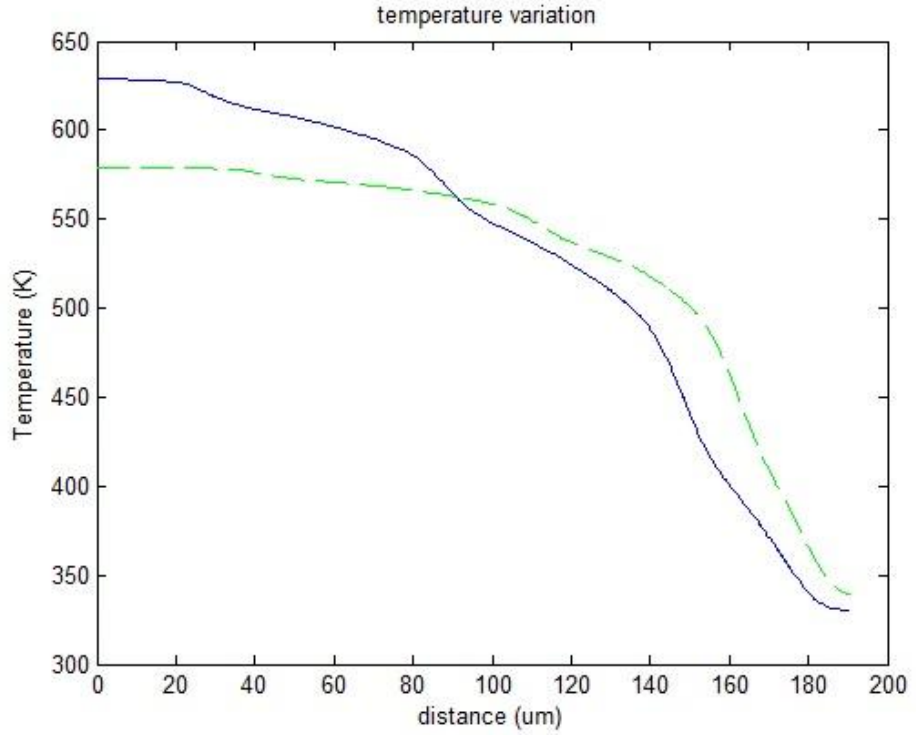

Fig. 5.5.5 Temperature variation along the line between two terminals of double meander shape microheater.

Table 5.1 shows the analysis and comparison of the S-shape and double meander shape microheaters.

Table 5.1: *Analysis of MEMS microheater.*

Geometry	**Maximum Temperature (K)**	**Temperature Uniformity**
Double meander uniform width	628.68	~ 40%
Double meander non uniform width	579.15	~ 60%
s-shaped uniform width	567.43	~70%
s-shape non uniform width	588.47	~80%

From the simulation results and the comparison table it is clear that S-shape varying width microheater shows better temperature uniformity. So this s-shape microheater is used for calculating further results.

Gas Detection

In presence of heat the ambient gases reacts with the sensing layer. It either oxidizes or reduces the sensing layer. This reaction changes the resistivity of the sensing layer which is detected by the IDT. Whenever the resistivity of the layer changes the resistance across the IDE terminals also changes and the result is observed. Fig. 5.5.6 shows a graph between the resistance across IDE's and the resistivity change of the sensing layer due to gas.

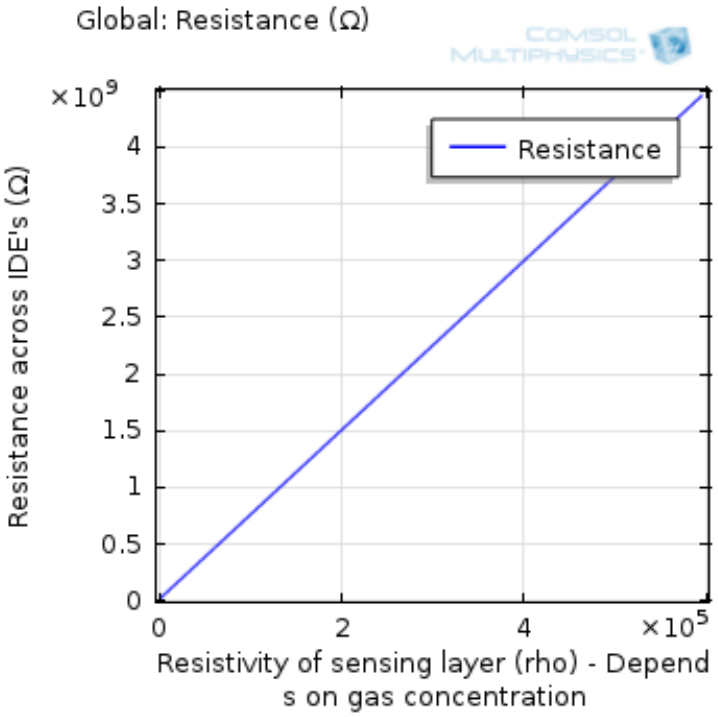

Fig. 5.5.6 Effect of resistivity change on resistance of IDT.

5.6 CONCLUSION

A comprehensive model of microheaters is designed and simulated. Comparison between double meander and s-shape microheaters is done and it is analyzed that S-shape microheater provide better temperature uniformity. Similarly, microheater geometries with different width are analyzed for temperature uniformity. It has been found that the varying width microheater shows better temperature uniformity than the uniform width microheater with same geometry. Also the resistance change across the IDE's with the change in the resistivity of sensing layer (depends on the presence of gas) is analyzed and discussed.

CHAPTER-6

FABRICATION STEPS

6.1 Fabrication steps of MEMS based gas sensor

For design of MEMS based gas sensor, Silicon <100> will be used used as substrate as material shown in Fig. 6.1.

Fig. 6.1 Silicon wafer <100> as substrate

Fabrication steps are as follows:

- Wafer cleaning
- Oxidation
- Lithography
- Platinum deposition
- Silicon nitride deposition (sputtering) and annealing
- Back side membrane patterning and Oxide Etching
- Silicon etching using TMAH solution
- Silicon nitride removal
- IDT deposition
- Deposition of Sensing layer

6.1.1 Wafer Cleaning

Generally, before using silicon wafer in fabrication process, it should be cleaned chemically to remove heavy metals, organic films and particulates. There are three different techniques available for cleaning.

- Piranha Cleaning
- RCA- 1 Cleaning
- RCA-2 Cleaning

For use any one technique, one should switch on the exhaust of chemical hood. Wear protective gown, goggle, mouth mask, head cap just before starting work on wet bench.

(A) Piranha Cleaning

Piranha solution which is used for cleaning purpose, is made of a mixture of H_2SO_4 (sulfuric acid) and H_2O_2 (hydrogen peroxide). As the mixture is a strong oxidizing agent, that will clean most of organic matter, also it will also hydroxylate partially all surfaces (add OH groups) and it is making them highly hydrophilic (water compatible).

There are many different mixture ratios utilized and all are commonly called piranha. A typical mixture is 3:1 concentrated H_2SO_4 (sulfuric acid) to 30% H_2O_2 (hydrogen peroxide); other protocols can be used a 4:1 or even 7:1 mixture. A closely related mixture, sometimes called "base piranha", is a 3:1 mixture of ammonium hydroxide (NH_4OH) with hydrogen peroxide. Piranha solution must be made with great precautions. It is very corrosive and also an extremely powerful oxidizer. Surfaces must be carefully cleaned, and totally free of organic solvents before coming into contact with piranha solution. Piranha solution makes clean by dissolving organic impurities, and a large amount of impurity will reason violent bubbling also a discharge of gas that can cause an explosion.

Piranha solution must be prepared by adding H_2O_2 (hydrogen peroxide) to H_2SO_4 (sulfuric acid) very slowly, never vice versa. This process will generate heat. The resultant heat can increase solution temperatures exceeding 100° C. Before applying any heat, it must be permissible to cool reasonably. The abrupt raise in temperature can also lead to violent boiling, or even spraying of the tremendously acidic solution. Explosions may occur if the peroxide solution concentration is higher than 50% of total solution. Once the mixture is become stable, it can be further heated to maintain its reactivity. The hot (often bubbling) solution will clean organic composites off substrates, and oxidize or hydroxylate most of surfaces. Cleaning usually requires about 10 to 40 minutes, after which time the substrates can be removed from the solution.

The solution may be mixed before application or directly applied to the material, applying the sulfuric acid first, followed by the peroxide. Due to the self-decomposition of hydrogen peroxide, piranha solution should be used freshly prepared. Piranha solution should not be stored. Immersing the substrate (such as a

wafer) into the solution should be done slowly to prevent thermal shock that may crack the substrate material.

(B) RCA- 1 Cleaning

Take 2 quartz beakers, 1 measuring cylinder, wafer holder and wash with DI (Deionised) water (DI water plant has been placed just next to the wet bench).

Preparation of RCA-1 solution:

RCA-1 is a solution of Deionised Water (DI H_2O): Ammonium hydroxide (NH_4OH): H_2O_2 (hydrogen peroxide) (5:1:1)

(Always add reactive compounds (acid/base) to water)

a.) 200 ml DIH_2O b.) 40 ml NH_4OH c.) 40 ml H_2O_2

Take 200 ml DI water into Cleaned beaker. Add 40ml H_2O_2 and 40ml NH_4OH to DI water. Once the solution is prepared, keep it on a hot plate. Turn on the hot plate and set temperature to 150° C. The solution will need to be heated to 80° C. This will take about 15 minutes. Once solution gets heated up to 80° C, load silicon wafer into wafer holder and immerse into heated RCA-1 solution for 15 minutes. After 15 minutes of cleaning take out wafers from the solution and rinse with DI water thoroughly for 1minute.

(C) RCA- 2 Cleaning

Preparation of RCA-2 solution:

RCA-2 is a solution of Deionised Water (DI H_2O): Hydrochloric acid (HCl): H_2O_2 (hydrogen peroxide) (6:1:1)

a) 240 ml DI Water b) 40 ml H_2O_2

c) 40 ml HCl

Take 240 ml DI water into Cleaned beaker .First Add 40ml H_2O_2 and then 40ml HCl to DI water. Once the solution is prepared, keep it on a hot plate. Turn on the hot plate and set temperature to 150° C. The solution will need to heat to 80° C. This will take about 15 minutes. Once solution gets heated up to 80° C, load silicon wafer into wafer holder and immerse into heated RCA-2 solution for 15 minutes. After 15 minutes of cleaning take out wafers from the solution and rinse with DI water thoroughly for 1minute. The RCA-2 cleaning removes metallic contaminants from the wafer.

Preparation of dilute HF (hydrofluoric acid solution):

Measure 200ml of DI water using measuring cylinder and pour into 250 ml polypropylene beaker and then measure 2ml of HF in a polypropylene measuring cylinder and add to DI water and mix thoroughly using Teflon rod. Then dip RCA2 cleaned silicon wafer into dilute HF solution for 15 seconds and finally rinse with DI water for 1min.

Now the wafers are ready for thermal wet oxidation process.

6.1.2 Oxidation

There are four different methods of oxidation as mentioned below:

1. Diffusion oxidation
2. Wet oxidation
3. High pressure oxidation
4. Plasma oxidation

Though all methods are effective but wet oxidation is used for MEMS based gas sensor fabrication process. Wet oxidation is explained in details as below:

Switch on the mains of thermal wet oxidation furnace to grow 1000 nm oxide layer. Ramp up furnace temperature to 500° C and pass nitrogen gas (0.5 liter/min) into the furnace to create inert nitrogen atmosphere. Then load the wafers into furnace and ramp up furnace temperature from 500° C to 1100° C. Now pass oxygen gas (1 liter/min) directly into the furnace for 10 minutes for dry oxidation. After 10 minutes stop direct supply of oxygen gas into the furnace and pass oxygen through the water bubbler (bubbler temperature should be 97° C) for 3hrs for wet oxidation. After 3hrs stop oxygen supply and pass nitrogen gas (0.5 liter/min).Ramp down the furnace temperature to 37° C and unload the wafers. This oxide is used as a hard mask during the Potassium Hydroxide (KOH)/TMAH etching process. After this step, we have structure as shown in Fig. 6.2.

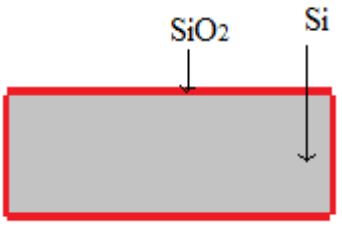

Fig. 6.2 Structure after wet oxidation

6.1.3 Lithography

Top side of oxidized wafer is coated with S1813 Photoresist at 4000 rpm for 40 seconds and prebaked at 125° C temperature for 1minute for top layer pattern transferring double sided EVG 620 mask aligner will be used used. The UV bulb is switched on for 10 minute for stabilization. Mask is loaded according to procedure (guided by software on the screen).

Wafer is loaded and aligned with the mask. Then the mask pattern is transferred onto the coated photoresist by UV exposure, the pattern is then developed in a MF26A developer solution for 1min and rinsed with DI water followed by nitrogen drying.

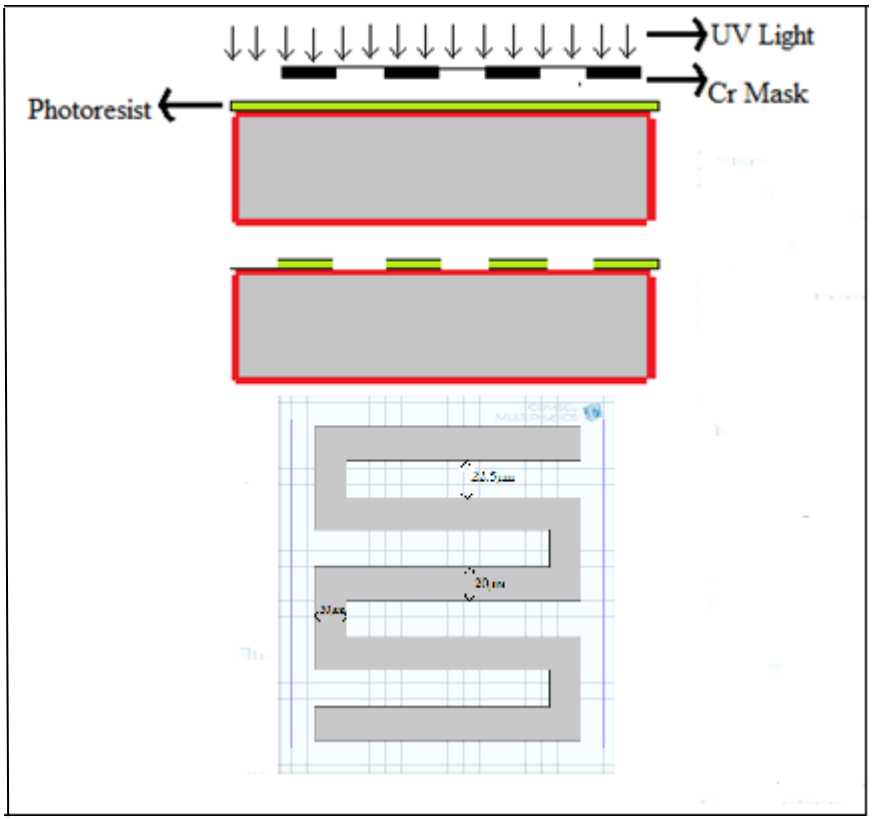

Fig. 6.3 Top view of mask lay out design of micro-heater with dimension.

6.1.4 Platinum deposition

200nm platinum was deposited after lithography process by sputtering method.

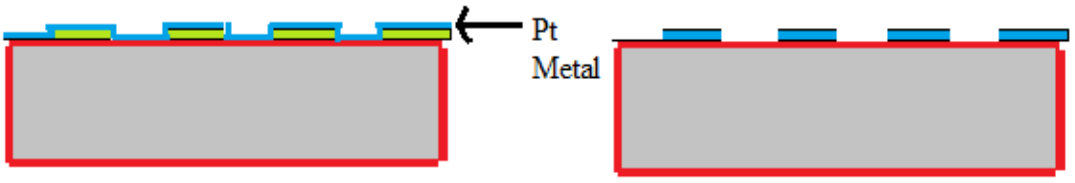

Fig. 6.4 Structure after Platinum deposition.

Standard Sputtering parameters used in prior are:

Plate voltage: 1.5 KV

Incident power: 60w Reflected power: 25W

Plate current: 60mA

Distance between target and substrate: 5.2cm

Pre sputtering time: 2min

Deposition time: 8min

6.1.5 Silicon nitride deposition (sputtering) and Annealing

80nm silicon nitride was deposited as a hard mask for bulk silicon etching.

Sputtering parameters: Plate voltage: 1.5KV Incident power: 60W Reflected power: 20W Plate current: 60mA

Distance between target and substrate: 6cm

Pre sputtering time: 15min

Deposition time: 15min

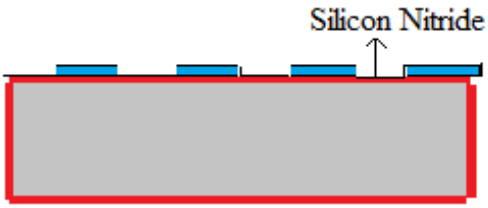

Fig. 6.5 Structure after Silicon Nitride deposition.

After deposition, nitride has to be annealed in a polymer annealing furnace at 700° C temperature for 45 min in nitrogen ambient. Flow rate of nitrogen should be 0.5 ltr/min.

6.1.6 Back side membrane patterning and Oxide Etching

Back side of oxidized wafer has to be coated with S1813 Photoresist at 4000 rpm for 40 seconds and prebake it at 125 degree temp for 1min. For membrane, pattern has to be aligned with respect to top layer pattern by double sided EVG 620 mask aligner.

The UV bulb is switched on for 10 min for stabilization.

The parameters set are: Soft Contact

Constant Dosage -75mJ/cm^2

Wafer is loaded and aligned with the mask

The mask pattern will be transferred onto the coated photoresist by UV exposure. The pattern is then developed in a MF26A developer solution for 1min and rinsed with DI water followed by nitrogen drying.

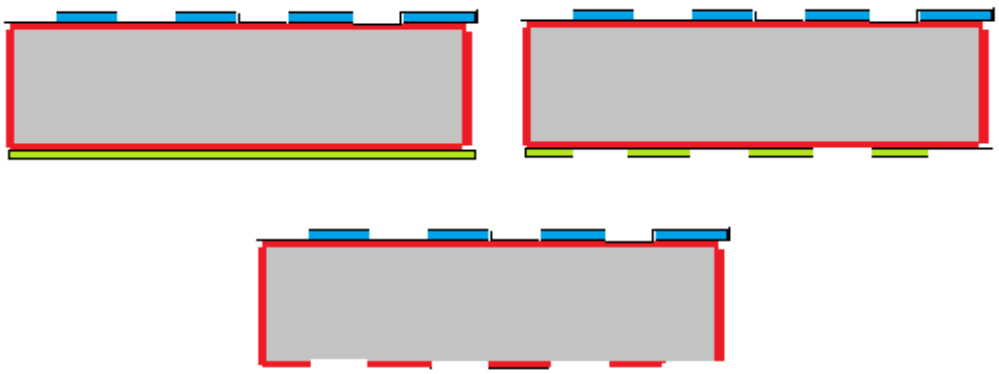

Fig. 6.6 Structure after membrane patterning and Oxide Etching

6.1.7 Silicon etching using KOH + IPA and TMAH solution

Preparation of 30% KOH solution

Weigh 105g of 85% pure KOH pellets into 250ml glass beaker and add 195ml of DI water and stir it thoroughly till KOH pellets dissolves completely. Keep this solution on a hot plate for heating to 75° C. Once after reaching temperature add 50ml of IPA to the heated KOH solution and immerse wafer into the solution for silicon etching for 2hrs and 30min after 2hrs and 30min etching take out wafer from the solution and wash with DI water thoroughly and dry with nitrogen. Etch rate of silicon in KOH+IPA is 50micron/ hour and etch rate of silicon oxide is 150nm / hour.

Preparation of 5% TMAH solution

Take 200ml of DI water in a clean 250ml beaker and then add 40ml of 25%TMAH solution. Once the solution is prepared, keep it on a hot plate .Turn on the hot plate and set temperature to 150° C. The solution will need to heat to 75° C. This will take about 15 minutes. Once solution gets heated up to 75° C, add 0.2g of ammonium persulphate salt to the solution. Load KOH+IPA etched silicon wafer into wafer holder and immerse into heated TMAH solution for 3 hrs for further silicon etching. Take out sample from the solution and rinse with DI water followed by methanol.

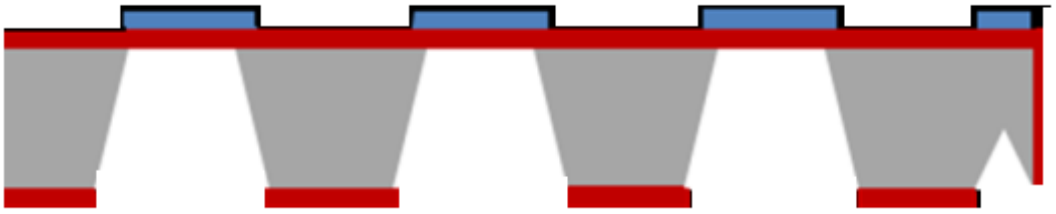

Fig. 6.7 Structure after Silicon etching using KOH + IPA and TMAH solution.

6.1.8 Silicon Nitride Removal

Silicon nitride was etched using 1:3 BHF solution by dipping for 10secs.After etching of silicon nitride layer wafer was thoroughly rinsed with DI water and dried with nitrogen.

Fig. 6.8 Structure after removal of Silicon Nitride.

6.1.9 IDT deposition

For deposition of IDT (Interdigitated Electrodes), there is same procedure followed which is used in micro-heater deposition. Generally, Au or/and Ag materials are used for IDT. Use of IDT is to detect resistance change of sensing surface.

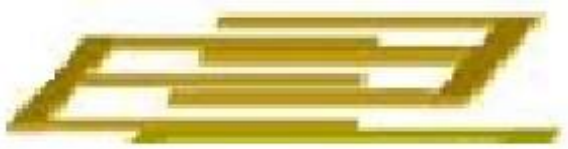

Fig. 6.9 IDT structure for detection of resistance change of sensing surface

6.1.10 Deposition of Sensing Layer

On IDT electrodes, sensing surface is deposited. Typically, Tin oxide (SnO_2), Zinc oxide (ZnO), Tungsten trioxide (WO_3), Indium tin oxide (ITO), Titanium oxide (TiO_2), Cerium oxide (CeO_2) are used for sensing surface.

CHAPTER-7

CONCLUSION AND FUTURE PROSPECTS

7.1 Summary

The work presented in this thesis includes the simulation results of the microheater. It was aimed at improving the temperature uniformity of the microheater which is used in a gas sensor. Different materials to be used for microheater were studied. ZnO has been chosen for the sensing layer and Pt for heater. Different microheater geometries were observed and simulated to improve the overall temperature uniformity. The effect of presence of a gas is studied in the form of resistance change across IDT. FEM method is used for simulation using COMSOL Multiphysics.

7.2 Conclusion

In the present work, a MEMS based microheater for gas sensing application has been studied. The method used and the results have provided the design rules and criteria for FEM method analysis. Microheaters are based on the principal of joule heating. Different geometries were simulated to observe the heating profile and to obtain the desired temperature. By varying the dimensions of the heater we obtained more temperature uniformity. Out of all the geometries analyzed S-shape microheater provides maximum temperature uniformity and when the dimensions were varied the result was significantly improved. The heater was placed on an insulating base of SiO_2 and the heater is made of platinum. Also an IDT is placed coplanar to the microheater to detect the changes in the environment. Upon the heater is a sensing layer made of ZnO which is sensitive to gases in the presence of heat. By applying a voltage of 0.5V we obtained a temperature of 588.47^{o} K. Also by varying the resistivity of the sensing layer (in presence of gas) we observed the change in resistance across IDE's.

7.3 Future Scope

In future no doubt Pt will be used for microheater material but still a lot more research is needed to choose better material for the microheater. Dilver P1 (composition of alloy like Fe, Ni and Co) is considered available option as it consumes less power and has good resistivity, though it generates less temperature as compared to Platinum. There is also scope in modification of the sensor layer to have better response magnitude and time according to the requirements. Research is also possible for more low power consumption heaters that can be used industrially and can serve better longevity. The signal processing unit can also be developed for giving a sensor alarm.

REFERENCE

[1] M. Mehregany, "Microelectromechanical system", *Circuit and Devices Magazine IEEE*, vol. 9, no. 6, pp. 14-22, July 1993.

[2] Stephen D. Senturia, *Microsystem Design*, London: Kluwer Academic Publishers, November 2000.

[3] *"What is MEMS Technology?"*, www.mems-exchange.org

[4] *An Introduction to MEMS*, PRIME Faraday Partnership, Loughborough University, Loughborough, U.K., 2003.

[5] Zaini Abdul Halim, "Design of Microhotplate Based Gas Sensing System", *Ph.D Thesis*, Electrical & Electronic Engineering Department, Universiti Sains Malaysia, May 2008.

[6] R. Ghodssi and P. Lin, "MEMS Materials and Processes Handbook", *Springer*, New York, London, 2011.

[7] K. Arshak, E. Moore, G.M. Lyons, J. Harris and S. Clifford, "A review of gas sensors employed in electronic nose applications", *Sensor Review*, vol. 24, no. 2, pp.181-198, November, 2004.

[8] T.C. Pearce, S. S. Schiffman, H.T. Nagle, and J. W. Gardner, *Handbook of Machine Olfaction*, Wiley-VCH, Weinheim, 2003.

[9] Frank Rock, Nicolae Barsan, and Udo Weimar, "Electronic Nose: Current Status and Future Trends", *Chemical Reviewer*, vol. 108, pp. 705-725, August 2008.

[10] Fauzan Khairi Che Harun, Andik Marwintan Jumadi and Nasrul Humaimi Mahmood, "Carbon black polymer composite gas sensor for electronic nose", *International Journal of Scientific & Engineering Research*, vol. 2, no. 11, November 2011.

[11] Alphus D. Wilson 1, and Manuela Baietto, "Applications and Advances in Electronic-Nose Technologies", *Sensors*, vol.9, pp. 5099-5148, June 2009.

[12] Seokheun Choi, Simeng Chen, Yuchao Wang, " Applications and Technology of Electronic Nose for Clinical Diagnosis", *Open Journal of Applied Biosensor*, vol. 2, pp. 39-50, May 2013.

[13] Paul E. Keller, Lars J. Kangas, Lars H. Liden, Sherif Hashem, Richard T. Kouzes, "Electronic noses and their applications", *Proceedings of IEEE Northcon/Technical Applications Conference (TAC'95),* Portland, OR, USA, 12 October 1995.

[14] J. W. Gardner, E. L. Hines, and M. Wilkinson, *"*Application of Artificial Neural Networks to an Electronic Olfactory System*"*, *Measurement Science and Technology*, vol. 1, pp. 446-451, November 1990.

[15] David Tin Win, "The Electronic Nose – A Big Part of Our Future", *AU J.T.*, vol. 9, no. 1, pp. 1-8, July 2005.

[16] K. Wetchakuna, T. Samerjaia, N. Tamaekonga, C. Liewhirana, C. Siriwonga, V. Kruefua, A. Wisitsoraatb, A. Tuantranontb and S. Phanichphanta, "Semiconducting metal oxides as sensors for environmentally hazardous gases.", *Sensors and Actuators B*, vol.160, pp. 580– 591, August 2011.

[17] George Preti, Thomas S. Gittelman, Paul B. Staudte and Preston Luitweiler, "Letting the nose lead the way: malodorous components in drinking water", *Analytical Chemistry*, vol. 65, no. 15, pp. 699A-702A, August 1993.

[18] T.V. Belysheva, L.P. Bogovtseva, E.A. Kazachkov and N.V. Serebryakova, "Gas-sensing properties of doped In_2O_3 films as sensors for NO_2 in air", *Journal of Analytical Chem*estry, vol. 58, no. 6, pp. 583–587, 2003.

[19] Kane Jonathan Miller, "Simulation and fabrication of microhotplates for metal oxide gas sensors", *M.Tech Dissertation*, Chemical Department, B.S. University of Louisville, August 2010.

[20] Kraig D. Mitzner, Jason Sternhage and David W. Galipeau, "Development of a micromachined hazardous gas sensor array", *Sensors and Actuators B,* vol. 93, pp.92-99, 2003.

[21] Jack W Judy, "Microelectromechanical systems (MEMS): fabrication, design and applications".

[22] H. Meixner, U. Lampe, “Metal oxide sensors”, *Sensors and Actuators B 33* (1996), 198-202.

[23] Isolde Simone, Nicolae Bârsan, Michael Bauer, Udo Weimar, “Micromachined metal oxide gas sensors: opportunities to improve sensor performance”, *Sensors and Actuators b 73 (2001) 1-26.*

[24] T Seiyama, A. Kato, K. Fujushi, m. Nagatani, “A new detector for gaseous component using semiconductive thin films”, *Anal. Chem. 34 (1962) 1502f.*

[25] Figaro products Catalogue, Figaro gas sensors 2000-series, *Figaro Engineering Inc.*

[26] FIS, Product list (specifications:Sb/sp), *FIS incorporated*, May 1999.

[27] K. Schierbeum, U. Weimar, W. Göpal, “Multicomponent analysis: an analytical chemistry approach applied to modified SnO2 sensors”, *Sens Actuators B 2 (1990) 71-78.*

[28] J. Cerdà Belmonte, J. Puigcorbe, J. Arbiol , A.Vila, J. R. Morante, N. Sabate, I. Gracia and C. Cane, “ High-temperature low-power performing micro machined suspended micro-hotplate for gas sensing applications”, *Sensors and Actuators B*, vol. 114, pp. 826–835, 2006.

[29] J Puigcorbé, D Vogel, b Michel, A Vilà, A grácia, C Cané, “ Thermal and mechanical analysis of micromachined gas sensor”, *J. Micromech. Microeng, 13(2003) 548-556.*

[30] Carole Rossi, Pierre Temple-Boyer, Daniel Esteve, “Realization and performance of thin SiO2/SiNx membrane for microheater applications”, *Sensors and Actuators A 64 (1998) 241-245.*

[31] Carole Rossi, Emmanuel Scheid, Daniel Esteve, “Theoretical and experimental study of silicon micromachined microheater with dielectric stacked membranes”, *Sensors and Actuators A 3 183-18.*

[32] Gotz A, Gracia I, Cane C, Lora-Tamayo E “Thermal and mechanical aspects for designing micromachined low power gas sensor”, *J. Micromech. Microeng,* 1997,*247-9.*

[33] S. M. Lee, D C Dyer J W Gardner, “Design and optimization of a high

temperature silicon micro-hotplate for nanoporous palladium pallistors", *Microelectronics Journal 34 (2003) 115-126.*

[34] S. Roy, T. Majhi, A. Kundu, C. K. Sarkar, and H. Saha, "Design, Fabrication and Simulation of Coplanar Microheater Using Nickel Alloy for Low Temperature Gas Sensing Application", *Sensor Letters, vol. 9, pp. 1382–1389, 2011*.

[35] L. Sujatha, V. S. Selvakumar, S. Aravind, R. Padamapriya, B. Preethi. "Design and Analysis of Micro-Heaters using COMSOL Multiphysics for MEMS Based Gas Sensor", *Proceedings COMSOL Conference*, India, 2012.

[36] G. Velmathi, N. Ramshanker and S. Mohan, "2D Simulations and Electro-Thermal Analysis of Micro-Heater Designs Using COMSOLTM for Gas Sensor Applications", in *Proceedings of the COMSOL Conference*, India, 2010.

[37] S. Semancik, R.E. Cavicchi, M.C. Wheeler, J.E. Tiffani, G.E. Poierier, R.M. Walton, J.S. Suehle, B. Panchapakesan and D.L. De Voe, "Microhotplate platforms for chemical sensor research", *Sensors and Actuators B*, vol. 77, pp. 579–591, 2001.

[38] Bijoy kantha, Pallavi kar, Saral saha and Subir Kumar sarkar, "Design and Electro- Thermal Analysis of MEMS based Micro-hotplate for Gas Sensor", *Chennai and Dr. MGR University Second International Conference on Sustainable Energy and Intelligent System,* 2011.

[39] G. Velmathi, N. Ramshanker and S. Mohan, "2D Simulations and Electro-Thermal Analysis of Micro-Heater Designs Using COMSOLTM for Gas Sensor Applications", in *Proceedings of the COMSOL Conference*, India, 2010.

[40] Jae-Cheol Shim, Gwiy-Sang Chung, "Fabrication and Characteristics of Pt/ZnO NO Sensor Integrated SiC Micro Heater*", IEEE SENSORS Conference*, India, 2010.

[41] *Introduction to COMSOL Multiphysics users manual*, Oct. 2012.

[42] Chris Long & Naser Sayma, "Heat Transfer Module", *Venture Publishing AsP*, 2009.

[43] *Introduction to Structural Mechanics Module users manuals*, May 2012.

[44] S. M. Lee, D.C. Dyer and J. W. Gardner, "Design and optimization of a high-temperature silicon micro-hotplate for nanoporous palladium pellistors", *Microelectronics Journal,* vol. 34, pp.115–126, 2003.

[45] Lie-yi Sheng, Zhenan Tang, Jian Wu, Philip C.H. Chan and Johnny K.O. Sin, "A low-power CMOS compatible integrated gas sensor using maskless tin oxide sputtering", *Sensors and Actuators B*, vol. 49, pp. 81–87, 1998.

[46] Indrajit Singh and S. Mohan, "3D simulation and elecro-thermal analysis of micro- hotplate design using CoventorWare for MEMS based gas sensor application", *International conference on smart material structures and systems*, pp. 28-30, 2005.

[47] J. Jakovenkoa, T. Lalinsky, M. Drzik, M. Ivanova, G. Vankob and M. Husak, "GaN, GaAs and Silicon based Micromechanical Free Standing Hot Plates for Gas Sensors", *Chemistry 1*, pp. 804–807, 2009.

[48] V. K. Khanna, Mahanth Prasad, V. K. Dwivedi, Chandra Sekhar, A. C. Pankaj and J. Basu, "Design and Electro-Thermal Simulation of a Polysilicon micro-heater on suspended membrane for use in gas sensing", *Indian Journal of Pure and Applied Physics*, vol. 45, pp. 332-335, April 2007.

[49] S.S.Mondal, S.Roy, C.K.Sarkar, "Design and Electrothermal analysis of MEMS based Microheater Array for Gas Sensor using INVAR alloy", *International Conference on Communications, Devices and Intelligent Systems (CODIS),* 2012.

APPENDIX-I

Material properties used in simulation

Sr. No.	Properties	SiO_2	Platinum
1.	Co efficient of thermal expansion in 1/K	0.5e-6	8.80e6
2.	Heat capacity at constant pressure in J/kg-K	730	133
3.	Relative permittivity	4.2	7.0
4.	Density in kg/m^3	2200	21450
5.	Thermal Conductivity in W/m-K	1.4	71.6
6.	Young's modulus in Pa	70e9	168e9
7.	Poisson's ratio	0.17	0.38
8.	Electrical Resistivity in Ω-m	10e18	10.6e-8

LIST OF PUBLICATION

- Mayank Dhull, Anil Arora, "Design of MEMS Based Microheater for Enhanced Efficiency of Gas Sensors", *Journal of Thermal Engineering and Application* 2015; 2(2).